8-21-2015 12:00 AM

Developing a contrast agent for the in vivo detection of apoptosis

Mary R. Cobb, *The University of Western Ontario*

Supervisor: Dr. Stephen Pasternak, *The University of Western Ontario*
Joint Supervisor: Dr. Robert Bartha, *The University of Western Ontario*
A thesis submitted in partial fulfillment of the requirements for the Master of Science degree in Neuroscience

DEVELOPING A CONTRAST AGENT FOR THE *IN VIVO* DETECTION OF APOPTOSIS

(Thesis format: Monograph)

by

Mary Rebecca Cobb

Graduate Program in Neuroscience

A thesis submitted in partial fulfillment
of the requirements for the degree of
Master of Science

The School of Graduate and Postdoctoral Studies
The University of Western Ontario
London, Ontario, Canada

Abstract

Currently, there is no way to assess apoptotic cell death in living organisms. We have developed a novel contrast agent targeted toward the detection of caspase-3 activity, the key enzymatic mediator of apoptosis. Our contrast agent consists of a dual magnetic resonance imaging/fluorescent probe coupled to a cell penetrating peptide (CPP) sequence by a peptide backbone containing a caspase-3 cleavage site. The CPP allows the agent to cross cell membranes and the blood brain barrier. In cells undergoing apoptosis, activated caspase-3 will cleave the agent removing the CPP and trapping the imaging probes inside the cell.

The purpose of this study was to test the ability of our contrast agent to label apoptotic cells in cultured neurons and to explore its potential to detect apoptosis *in vivo*. Using multiple methods, we demonstrated that our contrast agent selectively labeled apoptotic but not healthy or necrotic neurons in culture. Furthermore, using a caspase-3 inhibitor we demonstrated that uptake and retention of the contrast agent was dependent on apoptosis and caspase-3 activation.

To test our contrast agent *in vivo*, we examined the 1-methyl-4-phenyl-1,2,3,6-tetrahydropyridine mouse model of Parkinson's disease to induce apoptosis in the dopaminergic neurons of the substantia nigra. At the time the mice were sacrificed, there was little evidence of apoptosis in the substantia nigra and we were not able to identify any cells with significant retention of the agent. Nonetheless, this data demonstrates that our agent effectively detects apoptosis in cultured neurons and reinforces its potential to image apoptosis *in vivo*.

Keywords:

Apoptosis, caspase-3, molecular imaging, contrast agent, MRI, fluorescent probe, cellular imaging

Acknowledgments

I would like to extend my gratitude to everyone who has helped me throughout the course of my thesis. First and foremost, I would like to thank Dr. Pasternak. Thank you for the guidance and mentorship you have provided over the past three years. Your enthusiasm for research and perpetual optimism are contagious and I don't know if I could have made it through to the end of this project without it. I would also like to thank my co-supervisor Dr. Bartha for his support, especially in the area of neuroimaging. I would like to extend a special thanks to Dr. Cregan, for continually offering up his expertise in the area of programmed cell death and for taking the time to help me with the MPTP mouse model. Without your help this project would not have been possible.

Fabiana Caetano, thank you for training me on the microscope and always being there to answer my questions with a smile on your face. Caroline O'Neil, thank you for all of your help with my histology – there is no way I would have found the substantia nigra without your help.

To my lab members - you have been a pleasure to work with and I have greatly enjoyed getting to know you. Thank you for providing an awesome work environment and exposing me to so many different cuisines and restaurants around London. An extremely special thanks goes out to Claudia, you are an amazing teacher and I would have never made it this far without your help. I would also like to thank Jon for helping me inject my mice with the contrast agent. I know how busy you are and I greatly appreciated you taking the time out of your day to help me.

Table of Contents

List of Figures

List of Abbreviations

AD:	Alzheimer's Disease
BBB:	Blood Brain Barrier
CA:	Contrast Agent
CAD:	Caspase-Activated Deoxyribonuclease
CNS:	Central Nervous System
CT:	Computed Tomography
DAB:	Diaminobenzidine
DAPI:	4',6-Diamidino-2-Phenylindole
DISC:	Death-Inducing Signaling Complex
DTPA:	Diethylene-Triamine-pentaacetate
^{18}F:	Fluorine-18
FDG:	Fluorodeoxyglucose
Gd:	Gadolinium
^{1}H:	Hydrogen
HD:	Huntington's Disease
H&E:	Hematoxylin and Eosin
^{123}I:	Iodine-123
ICAD:	Inhibitor of Caspase-Activated Deoxyribonuclease
^{111}In:	Indium-111

IP: Intraperitoneal

MAO-B: Monoamine Oxidase B

MCA: Middle Cerebral Artery Occlusion

MPP^+: 1-methyl-4-phenylpyridinium

MPT: Mitochondrial Permeability Transition

MPTP: 1-methyl-4-phenyl-1,2,3,6-tetrahydropyridine

MRI: Magnetic Resonance Imaging

MR: Magnetic Resonance

N2A: Neuro-2A

PARP: Poly ADP-Ribose Polymerase

PD: Parkinson's Disease

PET: Positron Emission Tomography

PI: Propidium Iodide

PS: Phosphatidyl Serine

SN: Substantia Nigra

SPECT: Single-Photon Emission Computed Tomography

^{99m}Tc: Technetium-99m

Tdt: Deoxynucleotidyl Transferase

TNF: Tumor Necrosis Factor

TUNEL: Terminal Deoxynucleotidyl Transferase-dUTP Nick End Labeling

Chapter 1

1 Introduction

Since its discovery in 1972 by Kerr *et al.*, the process of programmed cell death, otherwise known as apoptosis, has been intensely investigated. Years of research have gone into uncovering the molecular events and signaling pathways involved in this mode of cell death. Although we have come extremely far in the past 40 years, there is still no robust way of detecting apoptosis in living organisms. Additionally, there are limited techniques available to detect and label unfixed living apoptotic cells in culture.

This thesis presents a novel contrast agent for the *in vivo* detection of apoptosis. We present evidence in primary neuron culture that demonstrates the potential to allow the direct imaging of cells and tissues undergoing apoptosis in intact animals and humans. This imaging technique may prove to be very useful in the assessment of neuronal injury or the early diagnosis of neurodegenerative disease.

The following chapter reviews the process of programmed cell death or apoptosis, discusses common cell culture and mouse models used to investigate apoptosis and highlights current methods available for detecting apoptosis *in vitro* and *in vivo.* Finally, the chapter concludes with an introduction and description of our novel contrast agent for the *in vivo* detection of apoptosis.

1.1 Apoptosis

1.1.1 Overview of Programmed Cell Death

Apoptosis, or programmed cell death, is a regulated form of cell death that results in the systematic destruction and removal of a cell (Elmore, 2007). In contrast to necrosis, or accidental cell death, apoptotic cells play an active role in their own demise. Cellular destruction is carried out by an energy-dependent mechanism, involving a molecular

cascade of enzymes and proteases (Zimmermann and Green, 2001). Apoptosis is characterized by a series of morphological events, including cell shrinkage, chromatin condensation and nuclear fragmentation (Kerr et al., 1972). During the later stages of apoptosis the cellular and nuclear contents are packaged into membrane-bound vesicles called apoptotic bodies (Savill, 1997). The apoptotic bodies bud from the cell surface and are subsequently engulfed by surrounding macrophages and scavengers (Platt et al., 1998). Due to the controlled nature of this form of cell death, the cell is destroyed and removed without releasing its cellular contents into the extracellular space, avoiding any unwanted immune response (Savill and Fadok, 2000).

1.1.2 Caspases: The Mediators of Apoptosis

Caspases are a family of cysteine proteases that orchestrate the process of programmed cell death. They are synthesized in all cells and exist as inactive zymogens within the cytoplasm (McIlwain et al., 2013). In their inactive form, they contain a variable length pro-domain followed by a large and small subunit. Cleavage and subsequent release of the pro-domain causes activation of the caspase (Cohen, 1997). Activated caspases recognize specific tetrapeptide sequences on their substrates. Once activated, they cleave other caspases and downstream substrates after aspartic acid residues (Stennicke and Salvesen, 1998).

The caspases involved in apoptosis can be divided into two main groups: initiator caspases and effector caspases. The initiator caspases-8 and -9 are the primary caspases responsible for propagating the apoptotic signal through the apoptotic cascade and activating the pro-forms of the effector caspases (McIlwain et al., 2013). Once caspase-8 and -9 have been activated, they quickly cleave the effector caspases resulting in their activation (Stennicke et al., 1998; Slee et al., 1999).

The effector caspases are the central mediators of apoptosis: they are responsible for causing the morphological and biochemical changes seen in apoptosis. The effector caspases include caspase-3, -6, and -7, however, caspase-3 is considered the most

important executioner (McIlwain et al., 2013). Caspase-3 recognizes its substrates based on the tetrapeptide sequence DEVD (Stennicke and Salvesen, 1998). Once activated, caspase-3 is responsible for cleaving, and thereby activating, the enzymes that will dismantle and destroy the cell (Nicholson, 1999). Once caspase-3 has been activated within a cell, it is committed to die.

1.1.3 Molecular Signaling Pathways of Apoptosis

Apoptosis is a highly complex process involving alternate signaling pathways and numerous proteins and enzymes. There are a number of different ways to trigger apoptosis, and as a result, there are different signaling pathways that can be activated. The two main apoptotic pathways are the extrinsic or death receptor pathway and the intrinsic or mitochondrial pathway (Fig. 1). These two pathways eventually converge on a common pathway resulting in the activation of caspase-3, the key mediator of apoptosis (Zimmermann and Green, 2001).

1.1.3.1 Extrinsic Pathway

As the name suggests, the extrinsic pathway or death receptor pathway involves the binding of extracellular death ligands to their respective death receptors at the cell surface. The death receptors involved in this pathway are members of the tumour necrosis factor (TNF) receptor superfamily. These receptors all contain what is known as the death domain – a cytoplasmic domain that allows the death receptor to transmit the apoptotic signal from the extracellular environment to the intracellular environment (Ashkenazi, 2002). Some of the main death receptors and their respective ligands include FasR/FasL, TNF-α/ TNFR1, Apo2L/DR4 and Apo2L/DR5 (Nair et al., 2014).

Binding of a death ligand to its respective receptor results in the clustering and recruitment of adapter proteins on the cytoplasmic side of the receptor (Kischkel et al., 1995). This activity results in the formation of a complex called the death-inducing signalling complex (DISC) that incorporates caspase-8. Formation of DISC results in the autocatalytic activation of caspase-8 (Medema et al., 1997). Activated caspase-8 then

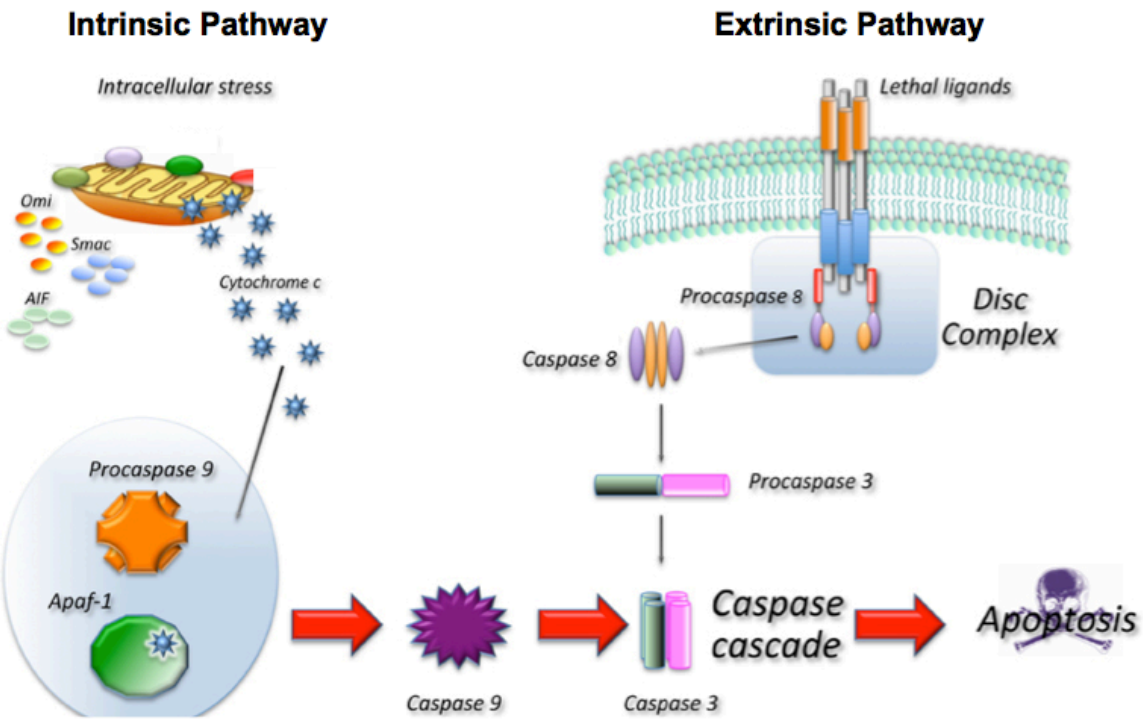

Figure 1. Schematic representation of the two main apoptotic pathways. In the extrinsic pathway binding of an extracellular death ligand to its respective death receptor leads to the formation of the DISC complex and activation of caspase-8. In the intrinsic pathway intracellular stressors lead to the release of cytochrome c from the mitochondria and the formation of the apoptosome and activation of caspase-9. Caspase-8 and caspase-9 activate caspase-3 leading to the destruction of the cell. Adapted from impactaging.com.

proceeds to propagate the apoptotic signal by cleaving and activating the executioner caspase-3 (Stennicke et al., 1998).

1.1.3.2 Intrinsic Pathway

The intrinsic or mitochondrial pathway is initiated through mitochondrial sensors for cellular distress. A variety of insults can disrupt mitochondrial function and activate this

pathway. These include the withdrawal of growth factors or hormones, radiation, toxins, hyperthermia, oxidative stress or DNA damage (Harmon et al., 1990; Clutton, 1997; Wadia et al., 1998; Watters, 1999). All of these insults are able to induce changes in the inner mitochondrial membrane that result in the opening of the mitochondria permeability transition (MPT) pore and loss of transmembrane potential (Green and Kroemer, 2004). Loss of the mitochondrial transmembrane potential causes the release of cytochrome c and other pro-apoptotic proteins from the intermembrane space of the mitochondria. The release of these proteins allows the formation of a caspase-activating structure called the apoptosome. The apoptosome is a large multimeric protein structure that incorporates and is responsible for activating caspase-9 (Zou et al., 1999). Following the formation of the apoptosome, activated caspase-9 proceeds to cleave and activate caspase-3, propagating the apoptotic signal through the pathway (Slee et al., 1999).

1.1.3.3 Execution Pathway

Activation of caspase-3 marks the end of both the extrinsic and intrinsic apoptotic pathways and the beginning of the execution pathway and degradation phase. It is during this phase that the cellular proteins responsible for dismantling and packaging up the cell become activated (Elmore, 2007). Once caspase-3 has been activated, the typical series of morphological changes leading to destruction and removal of the cell take place. These include cell shrinkage, chromatin condensation, nuclear fragmentation, plasma membrane blebbing, and finally the formation of apoptotic bodies (Kerr et al., 1972; Ziegler and Groscurth, 2004).

Caspase-3 is responsible for activating the proteolytic enzymes that will dismantle and destroy the cell. For example, caspase-3 is responsible for activating caspase-activated deoxyribonuclease (CAD), which will breakdown and degrade chromosomal DNA. CAD exists in the cytoplasm of cells as a complex with the inhibitor of caspase-activated deoxyribonuclease (ICAD). In apoptotic cells, caspase-3 cleaves ICAD releasing and activating CAD (Sakahira et al., 1998). Caspase-3 also activates enzymes and proteases that will degrade the cytoskeleton and nuclear lamina. Another substrate of caspase-3 is

gelsolin, an actin-binding protein that regulates actin filament assembly and disassembly. In apoptotic cells, cleavage of gelsolin by caspase-3 leads to disruption of the actin cytoskeleton contributing to the morphological changes observed in apoptosis (Kothakota et al., 1997).

1.1.4 Morphological and Biochemical Hallmarks of Apoptosis

Due to the regulated nature of apoptosis, cells undergoing this mode of cell death follow a typical sequence of morphological changes that lead to the destruction of the cell (Kerr et al., 1972). The first morphological change that can be observed in apoptotic cells is retraction and rounding up of the cell body. In the earliest stages of apoptosis the cell severs attachments to other cells and the extracellular matrix. Proteolysis and destruction of the cytoskeleton by caspase-3 and its substrates contributes to cell rounding (Taylor et al., 2008). This process of retraction and rounding can be easily seen in adherent cells grown in culture.

Following retraction and rounding, there is a reduction in cell volume, referred to as cell shrinkage. The cytoplasm becomes more dense and the organelles become more tightly packed (Bortner and Cidlowski, 1998). In the nucleus, chromatin condensation, or pyknosis, occurs. Cells undergoing chromatin condensation display compact round nuclei and can be easily identified with a nuclear stain. In contrast, healthy cells exhibit oval-shaped nuclei with more diffuse staining (Saraste and Pulkki, 2000; Ziegler and Groscurth, 2004).

As apoptosis progresses, membrane blebbing and fragmentation of the nucleus occurs. Cytoplasmic protrusions extend outwards from the cell surface giving a ruffled appearance to the plasma membrane. In a process called karyorrhexis, the nucleus is broken up and becomes fragmented (Saraste and Pulkki, 2000; Ziegler and Groscurth, 2004). Like pyknosis, this is one of the major hallmarks of apoptosis and can be easily visualized with a nuclear stain.

During the final stages of apoptosis, intact organelles and nuclear content are packaged into sealed membrane vesicles called apoptotic bodies. These apoptotic bodies bud from the blebbing plasma membrane (Saraste and Pulkki, 2000; Ziegler and Groscurth, 2004). Finally, the apoptotic bodies and remaining cell fragments are engulfed and digested by macrophages and other phagocytes. This allows the cell to be completely degraded and removed while maintaining membrane integrity (Platt et al., 1998). This is essential in avoiding an unwanted inflammatory response that would result from the release of cellular contents into the extracellular space (Savill and Fadok, 2000).

In addition to the characteristic morphological changes that occur during apoptosis, apoptotic cells undergo a number of characteristic biochemical changes. One of the major biochemical hallmarks of apoptosis is the externalization of the phospholipid phosphatidyl serine (PS) to the outer leaflet of the plasma membrane. This is an early event in the apoptotic cascade, occurring before any major morphological changes (Martin et al., 1995). Under normal circumstances, PS is restricted to the inner leaflet of the plasma membrane (Balasubramanian and Schroit, 2003). In cells undergoing apoptosis, this phospholipid is externalized and acts as a recruitment signal that allows phagocytes to recognize and engulf the apoptotic cell (Fadok et al., 1992).

Another biochemical hallmark of apoptosis is the controlled degradation of nuclear DNA into small fragments of equal length. Within the nucleus, double-stranded DNA is digested into internucleosomal fragments of approximately 180 base pairs by endonucleases (Duke et al., 1983; Wyllie et al., 1984). These endonucleases produce double-stranded DNA fragments with blunt ends and single base 3’ overhangs (Alnemri and Litwack, 1990; Didenko and Hornsby, 1996). This process occurs after caspase-3 activation and contributes to nuclear pyknosis and fragmentation.

1.1.5 Differentiating Apoptosis from Necrosis

In terms of cell death, apoptosis is often compared to its counterpart necrosis. Apoptosis is an active process: it is a managed form of cell death that relies on an energy dependent

mechanism and involves a proteolytic cascade and caspase activation. In contrast, necrosis is a passive process: it is an unregulated and accidental form of cell death that is energy-independent (De Saint-Hubert et al., 2009). Necrosis can result from a number of different insults, such as metabolic failure or mechanical trauma (Majno and Joris, 1995).

Apoptosis and necrosis differ in their morphological and biochemical features. Apoptotic cells display a typical progression of morphological changes including cell shrinkage, nuclear condensation, nuclear fragmentation, and the formation of apoptotic bodies (Kerr et al., 1972; Saraste and Pulkki, 2000). Cellular organelles remain intact throughout the destruction process and nuclear DNA undergoes internucleosomal fragmentation (Wyllie et al., 1984; Elmore, 2007). Necrotic cells on the other hand undergo cell swelling which eventually ruptures the plasma membrane leading to cell lysis. In this uncontrolled form of cell death organelles are disrupted and irregular DNA fragmentation occurs (Trump et al., 1997).

Apoptosis and necrosis also differ in their resulting immune response. Cells undergoing necrosis quickly lose their membrane integrity. Loss of membrane integrity and consequent release of cellular content triggers an inflammatory response. In contrast, cells undergoing apoptosis maintain their membrane integrity throughout the entire death process. Without the release of cytosolic material and proteolytic enzymes an inflammatory reaction does not occur (Savill and Fadok, 2000).

1.1.6 Apoptosis in Physiology and Pathology

Programmed cell death plays an indispensible role during development and is crucial for maintaining cell populations and normal physiology in adult organisms (Brill et al., 1999; Miura, 2011). The ability to safely eliminate and destroy cells without initiating an immune response is of great use to a multicellular organism (Platt et al., 1998). The formation of the human hand highlights the essential role that apoptosis plays during development. During embryonic development, the human hand begins as a paddle-like structure. As development progresses, apoptosis is triggered in the cells that lie between

fingers, leading to the development of a hand with five separate digits (Mori et al., 1995). If apoptosis is not effectively initiated, congenital deformities may result. One such deformity is syndactyly, where two or more digits fail to separate and are left fused together (Chong, 2010). Apoptosis also plays an essential role in adult organisms. For example, the epithelial cells of the small intestine are continually renewing themselves. In order to make room for new cells, older cells must undergo apoptosis and die (Shmuel, 1992).

It is clear that programmed cell death is essential for multicellular organisms. However, the apoptotic process requires a delicate balance: too little or too much apoptosis can have detrimental effects on an organism. Too little apoptosis can lead to uncontrollable tumour growth (Wong, 2011). Under normal circumstances, DNA damage will lead to the violation of cell cycle checkpoints, triggering apoptosis and preventing the mutated or damaged cell from surviving. In cancer, cells are able to overstep cell cycle checkpoints and evade apoptosis (Levine, 1997; Agarwal et al., 1998; Roos and Kaina, 2006). The evasion of apoptosis is fundamental to tumour development and resistance to anti-cancer therapy (Wong, 2011).

At the other end of the spectrum, too much apoptosis can be just as detrimental. In the brain, where neurons are not capable of regenerating, an excess of apoptosis can have severe consequences. In stroke patients, the ischemic penumbra is a surrounding zone of brain tissue that is not as severely affected by the stroke. It receives just enough oxygen and nutrients to survive, but not enough for normal function. Hours to days after the stroke, some cells found within this region undergo apoptosis, leading to more neuron loss and cognitive damage (Choi, 1996; Broughton et al., 2009).

1.1.6.1 Apoptosis and Neurodegenerative Disease

An excess of apoptosis can also contribute to neurodegeneration and has been implicated in a variety of neurodegenerative disorders, including Alzheimer's disease (AD), Parkinson's disease (PD) and Huntington's disease (HD). AD is a chronic brain disorder

that is characterized by progressive cognitive impairment and memory loss. On a cellular level, it is associated with neurofibrillary tangles, amyloid plaques, the loss of synapses, and the death of hippocampal and cortical neurons (Querfurth and Laferla, 2010). A number of studies have demonstrated a role for apoptotic-related neuron loss in AD. Post-mortem examination of brain tissue from patients with AD demonstrates increased DNA damage and caspase activation in neurons associated with amyloid deposits (Su et al., 1994; Masliah et al., 1998). Additionally, it has been shown that exposure of cultured neurons to amyloid-β can induce apoptosis directly (Loo et al., 1993).

PD is a movement disorder that is characterized by the progressive loss of dopaminergic neurons within the substantia nigra (SN). By the time of death, individuals affected by PD have lost 50-70% of their dopaminergic neurons within the SN (Davie, 2008). Apoptosis has been implicated as an important mechanism for neuron loss in PD. Post-mortem examination of brain tissue from patients with PD implicate apoptosis-related DNA damage and gene activation in the loss of dopamine neurons of the substantia nigra (Mochizuki et al., 1996; Jenner and Olanow, 1998). Additionally, mouse models and cell-culture models of PD implicate caspase-dependent modes of cell death in the loss of dopaminergic nigral neurons (Viswanath et al., 2001).

HD is another movement disorder characterized by the expansion of the CAG repeat in the *huntingtin* gene. HD involves the degeneration of striatal neurons resulting in motor impairment and uncontrolled body movements (Roos, 2010). Like AD and PD, there have been a number of studies that implicate an apoptotic mechanism in the loss of neurons. Analyses of brain tissue from patients with varying grades of HD demonstrated apoptosis-related DNA fragmentation in neurons and oligodendrocytes throughout the striatum (Portera-Cailliau et al., 1995). Furthermore, transgenic mouse models of HD show neuronal loss and apoptotic DNA fragmentation in the same regions observed in human patients. This is in comparison to wild-type mice that show no evidence of apoptotic DNA fragmentation in the same regions (Reddy et al., 1998).

1.2 Models of Apoptosis

1.2.1 Inducing Apoptosis in Cell Culture

There are a variety of ways to trigger apoptosis and therefore there are a number of different ways to induce apoptosis in cells grown in culture. One of the most common methods to induce apoptosis is with the use of chemicals or drugs. A number of drugs that induce apoptosis have been discovered as the result of anti-cancer drug research efforts. Camptothecin is a pro-apoptotic drug that was isolated from plant extracts in the 1950's and found to have anti-tumour activity (Wall and Wani, 1996). The compound induces apoptosis by inhibiting the DNA enzyme topoisomerase I. This causes DNA damage in the cell leading to the induction of apoptosis (Liu et al., 1996). Doxorubicin and etoposide are also anticancer drugs that can induce apoptosis in culture. They inhibit topoisomerase II causing DNA damage and inducing cell death (Karpinich et al., 2002; Mizutani et al., 2005). Additional drugs include staurosporine and tunicamycin. Staurosporine is a protein kinase inhibitor that induces apoptosis (Tamaoki et al., 1986). Tunicamycin blocks N-linked glycosylation and causes endoplasmic reticulum stress-induced apoptosis (Shiraishi et al., 2006).

It is also possible to trigger apoptosis in culture using the death receptor pathway. There are a number of different death receptors and their respective ligands can be used to induce apoptosis. Additionally, cross-linking a death receptor with an agonist anti-body can be used to stimulate the extrinsic pathway and induce apoptosis. The anti-Fas antibody is routinely used to induce apoptosis via the death receptor pathway (Gottlieb et al., 1996).

Serum withdrawal is another method used to induce apoptosis in cells grown in culture. The loss of growth factors triggers apoptosis via the mitochondrial pathway (Charles et al., 2005). Radiation has also been found to induce apoptosis in cells grown in culture. Radiation-induced DNA damage triggers apoptosis in these cells, however, it should be noted that this method can also cause necrosis (Balcer-Kubiczek, 2012).

1.2.2 Mouse Models of Apoptosis

In order to study apoptosis *in vivo*, a number of mouse models have been developed. The mouse models that will be outlined in this section include the induction of hepatic apoptosis via the injection of anti-Fas antibody, treatment of mouse tumor cells with anti-tumor drugs, cerebral stroke models and the 1-methyl-4-phenyl-1,2,3,6-tetrahydropyridine (MPTP) mouse model of Parkinson's disease.

1.2.2.1 Fas-Mediated Hepatic Apoptosis

In 1993, Ogasawara *et al.* reported the lethal effect of the anti-Fas antibody in mice. Intraperitoneal injection of the anti-Fas monoclonal antibody was found to rapidly induce apoptosis in hepatocytes. Histological analysis revealed that the majority of hepatocytes displayed pyknotic nuclei only 2 hours after injection with the antibody. The induction of apoptosis was extensive and occurred extremely rapidly killing the majority of mice within 6 hours (Ogasawara et al., 1993).

The mouse model of Fas-mediated hepatic apoptosis is now the most frequently used model to study apoptosis (Blankenberg et al., 1999; Keen et al., 2005; Luo et al., 2005). This model provides an excellent method for rapidly inducing widespread apoptosis in living organisms. Quantitatively, 63.7% of cells in anti-Fas treated livers stained positive for activated caspase-3 compared to normal livers that had 18.3% positive staining (De Saint-Hubert et al., 2009).

1.2.2.2 Treatment of Tumor Models with Anticancer Drugs

Treatment of tumor bearing tissue in mice with anti-cancer drugs can be used to model apoptosis *in vivo*. Tumor xenograft models are commonly used to produce tumors in mice. Tumor cells are injected subcutaneously or intramuscularly leading to the development of a tumor (Morton and Houghton, 2007). Mice can then be treated with anti-tumor chemotherapeutic drugs, such as doxorubicin, to induce apoptosis in the tumor (Hossain et al., 2012). Orthotopic lymphoma models have also been used to model apoptosis *in vivo*. Orthotopic tumors can be initiated by the intravenous injection of

lymphoma cells. Treatment with doxorubicin causes massive tumor cell loss within 24 hours of treatment and almost complete tumor regression within 4 days (Mandl et al., 2004). Cyclophosphamide has also been used to treat lymphoma in mice. Histological analysis revealed virtually complete (>95%) apoptosis in tumors treated with cyclophosphamide compared to <5% apoptotic cells in untreated control tumors (Blankenberg et al., 1998).

1.2.2.3 Cerebral Stroke Models

In the hours to days following an ischemic stroke, some neurons within the penumbra undergo apoptosis (Broughton et al., 2009). A number of different mouse stroke models exist, providing a method to recreate ischemia-induced apoptosis. The most utilized stroke model in mice has been the middle cerebral artery (MCA) occlusion. The MCA can be occluded either transiently or permanently producing a stroke; however, apoptotic cell death has been found to be more extensive after transient occlusion (Love, 2003). Histological analysis has revealed that apoptosis peaks 24-48 hours after reperfusion in the transient stroke model (Linnik et al., 1995; Chen et al., 1997).

Cerebral stroke models provide a valuable tool for studying apoptosis *in vivo* within the central nervous system (CNS). A major limitation of this model is the mixture of necrosis and apoptosis that occurs after stroke. After ischemic stroke, the most severely affected area dies rapidly via necrosis and forms the ischemic core (Kaufmann et al., 1999). The combination of necrosis and apoptosis make it difficult to isolate apoptotic cell death.

1.2.2.4 1-Methyl-4-Phenyl-1,2,3,6-Tetrahydropyridine Mouse Model of Parkinson's Disease

The MPTP mouse model of Parkinson's disease provides a more "pure" method for studying apoptosis in the CNS. MPTP is a potent neurotoxin that selectively targets the dopaminergic neurons of the SN (Heikkila et al., 1984). It is a lipid-soluble compound that can easily penetrate the blood brain barrier (BBB). Once in the CNS, MPTP is taken

up by astrocytes and converted to its toxic form 1-methyl-4-phenylpyridinium (MPP^+) by monoamine oxidase B (MAO-B). MPP^+ is then released into the extracellular space and taken up by dopaminergic neurons via the dopamine transporter (Tipton and Singer, 1993). Once in the cell, MPP^+ acts to inhibit complex I of the electron transport chain, interfering with oxidative phosphorylation in the mitochondria (Watanabe et al., 2005).

Primary neuronal culture treated with MPP^+ display apoptotic nuclear morphology and stain positively for activated caspase-3 (Viswanath et al., 2001). Intraperitoneal (IP) injection of MPTP selectively destroys the dopaminergic neurons of the SN in mice and causes Parkinsonian-like symptoms. Tatton and Kish demonstrated that a total cumulative dose of 150 mg/kg of MPTP delivered over five consecutive days reproducibly induces apoptosis in the dopaminergic neurons of the SN in C57Bl mice. Histological analysis revealed apoptotic DNA fragmentation and chromatin condensation in the dopaminergic neurons of the SN. They found that apoptotic cell death was initiated 72 hours after the first MPTP injection and peaked 24 hours after the final injection (Tatton and Kish, 1997).

The same protocol used by Tatton and Kish can be replicated to provide a mouse model for apoptosis within the CNS. Neurons were documented to die primarily via an apoptotic mechanism and the time of peak cell death is well documented. A limitation of this method is the small size of the SN and limited number of dopaminergic cells found within the mouse brain.

1.3 Methods for Detecting Apoptosis *in Vitro*

Since apoptosis was first discovered in 1972, a variety of methods have been developed for detecting this unique form of cell death. These techniques utilize the morphological and biochemical changes that take place in apoptotic cells (Fig. 2). This section will review the current techniques available for detecting apoptosis *in vitro* and *in vivo*, highlighting the advantages and pitfalls of each technique.

1.3.1 Cytomorphological Detection

Using electron microscopy, Kerr *et al*. closely observed and characterized the morphological features exhibited by apoptotic cells. They noticed that these cells appeared to undergo a programmed form of cell death that followed a characteristic progression of morphological events. This was in contrast to what was seen traditionally in necrosis. Using electron microscopy, they observed the characteristic morphological features in multiple types of tissue samples from various organisms (Kerr et al., 1972).

Today, electron microscopy is considered the gold standard for identifying apoptotic cells based on nuclear morphology. Electron microscopy boasts extremely high spatial resolution that is ideal for detecting the ultrastructural changes seen in apoptosis (Martinez et al., 2010). The same cytomorphological features that Kerr *et al.* described in 1972 are still used as benchmarks to identify apoptotic cells. Nuclear fragmentation and the formation of apoptotic bodies can be used to identify late apoptotic cells (Fig. 2). High spatial resolution also makes it possible to detect some of the morphological changes associated with early apoptosis, such as chromatin condensation (Watanabe et al., 2002; Martinez et al., 2010). On the downside, electron microscopy is very expensive and requires a high degree of training. The labour and time involved in visualizing samples with electron microscopy makes screening large numbers of cells very difficult. Additionally, cells must be fixed in order to visualize with electron microscopy, making cells no longer viable after detection (Huerta et al., 2007).

While not as sensitive as electron microscopy, light microscopy and fluorescence microscopy have become the most popular methods for identifying apoptotic cells based on morphology. Using light microscopy, cells in culture and tissue samples can be stained with hematoxylin and eosin (H&E) to visualize apoptotic morphology. After fixation, it is possible to detect nuclear condensation and fragmentation as well as apoptotic bodies using H&E stains (Jolly et al., 1997). The ability to detect apoptotic cells can be improved with the use of fluorescent dyes and fluorescence microscopy. The

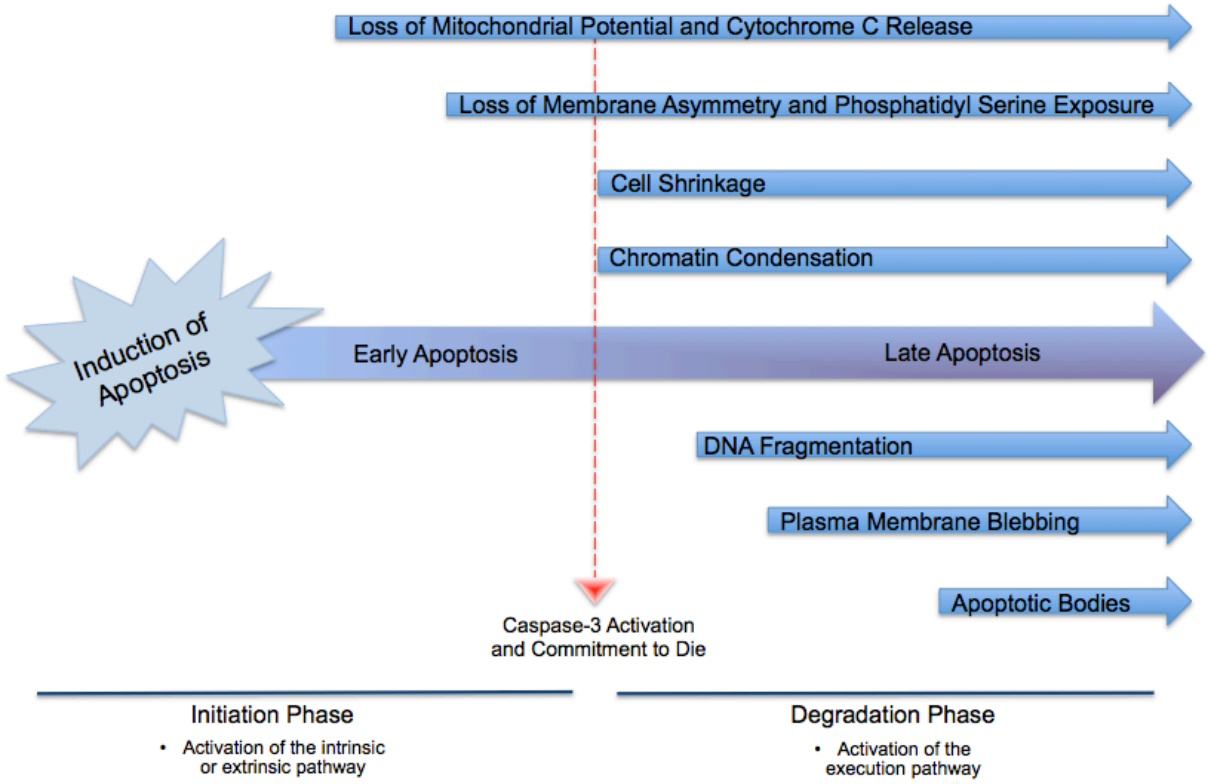

Figure 2. Time progression of the major morphological and biochemical events in apoptosis. A variety of methods have been developed to analyze apoptotic cell death based on the morphological and biochemical events that take place during apoptosis. Some assays target early apoptotic events, such as changes in the plasma membrane composition, and are useful for detecting early apoptosis. In contrast, some assays target late apoptotic events, such as DNA fragmentation, and are only capable of detecting late apoptosis.

use of fluorescent DNA-binding dyes like Hoechst 33342 make it much easier to identify pyknotic and fragmented nuclei. Hoechst 33342 is membrane permeable allowing researchers to stain living cells. Propidium iodide (PI) is a membrane-impermeable DNA-binding dye. It can be used in conjunction with Hoechst 33342 to exclude necrotic cells that have lost their membrane integrity, increasing specificity for apoptotic cells (Huerta et al., 2007). Due to the low spatial resolution of light microscopy and fluorescence

microscopy, it is only possible to detect late apoptotic cells that display considerable nuclear condensation and fragmentation (Fig. 2). Another limitation of light microscopy and fluorescence microscopy, as seen in electron microscopy, is difficulty in screening large numbers of cells. Additionally, electron microscopy, light microscopy and fluorescence microscopy are only able to capture apoptosis at a specific point of time. Apoptosis occurs in an asynchronous manner and proceeds rapidly once it has reached the degradation phase. As a result, it can be difficult to detect a large number of apoptotic cells using this method (Elmore, 2007; Huerta et al., 2007; Martinez et al., 2010).

1.3.2 DNA Fragmentation

Degradation of nuclear DNA into fragments of approximately 180 base pairs is a major biochemical hallmark of apoptosis. DNA is cleaved at internucleosomal sites by endonucleases that become activated by caspase-3 (Duke et al., 1983; Wyllie et al., 1984). Several methods have been developed to detect apoptosis based on DNA fragmentation. DNA laddering was developed to visualize DNA fragmentation when run on a gel. In this technique, genomic DNA is isolated from cells or tissue samples and electrophoresed on an agarose gel. Cells or tissues undergoing apoptosis will demonstrate a characteristic ladder of DNA fragments resulting from the regular cleavage of DNA at 180 base pair intervals (Daniel et al., 1999). This is in contrast to DNA isolated from necrotic cells, which demonstrate a smear when run on an agarose gel, resulting from random, non-uniform DNA degradation (Wyllie et al., 1984). DNA laddering is a good method for characterizing a population of cells as apoptotic; however, this technique has many limitations. In order to see the characteristic ladder, cells must be in the late stages of apoptosis, allowing enough time for adequate DNA fragmentation to take place (Collins et al., 1997). As a result, this method is not suitable for detecting cells in the early stages of apoptosis (Fig. 2). Another major disadvantage of DNA laddering is that it is qualitative and not quantitative. Laddering is only able to tell you if apoptosis is occurring in a population of cells and not the extent of apoptosis (Watanabe et al., 2002; Martinez et al., 2010).

In 1992, Gavrieli *et al*. developed the terminal deoxynucleotidyl transferase-dUTP nick end labelling (TUNEL) assay for the detection of apoptotic cells based on DNA fragmentation. In this technique, free 3'OH ends of DNA fragments are labelled enzymatically by terminal deoxynucleotidyl transferase (Tdt). The signal is then amplified and can be detected using light microscopy, fluorescence microscopy or flow cytometry (Gavrieli et al., 1992). The major advantage of this technique is the ability to provide *in situ* detection of DNA fragmentation. Using the TUNEL method, individual cells from tissue samples or culture can be identified as apoptotic. A variety of commercially available kits make this a quick and easy way to detect DNA fragmentation. The major disadvantage associated with this technique is that it is not completely specific to apoptosis. Random DNA fragmentation can occur in necrotic cells, resulting in false positives. Additionally, cells must be fixed prior to TUNEL staining, leaving cells no longer viable and making this an end point measurement (Elmore, 2007; Huerta et al., 2007; Martinez et al., 2010).

1.3.3 Annexin V

The externalization of PS from the inner leaflet to the outer leaflet during apoptosis is another major biochemical hallmark of apoptosis (Fadok et al., 1992). In 1994, Koopman *et al*. reported the ability of Annexin V to bind to externalized PS on the membrane of apoptotic cells. Annexin V is an endogenous anticoagulant protein that has an extremely high affinity for negatively charged phospholipids like PS (Tait et al., 1989). In the Annexin V binding assay, living cells are incubated with labeled Annexin V. Apoptotic cells that have externalized PS will bind labeled Annexin V allowing for detection using FM or flow cytometry (Koopman et al., 1994). A major limitation of this technique is that Annexin V alone is not able to discriminate between apoptosis and necrosis. The loss of membrane integrity is a defining feature of necrosis. Annexin V is consequently able to penetrate necrotic cells and label the inner leaflet of the membrane. In order to distinguish between apoptosis and necrosis, this assay requires the addition of a membrane impermeable nucleic acid dye such as propidium iodide (PI). PI will only label the nuclei of necrotic cells that have lost their membrane integrity, allowing for the

discrimination between apoptotic and necrotic cells (Annexin V positive and PI negative cells are classified as apoptotic; Annexin V positive and PI positive cells are classified as necrotic). Despite the inability of Annexin V to label and distinguish apoptotic cells on its own, this assay has some notable advantages. The first is the ability to observe apoptosis in living cells without the need of fixation. The second is the ability to detect cells in the early stages of apoptosis, as the externalization of PS to the outer leaflet is an early apoptotic event (Fig. 2) (Martin et al., 1995).

1.3.4 Detection of Apoptotic Mediators

The molecular cascade involved in the apoptotic pathway provides a number of targets for detecting apoptosis *in vitro*. Antibodies that target the cleaved form of caspase-3 or the cleavage products of caspase-3 substrates have been developed to detect apoptosis (Bressenot et al., 2009). These antibodies can be used in applications such as western blotting, immunocytochemistry, immunohistochemistry, and flow cytometry. Antibodies to the cleaved form of caspase-3 are commonly used to identify cells with activated caspase-3 in culture and tissue samples. Antibodies to the cleavage products of poly ADP-ribose polymerase (PARP), a direct substrate of caspase-3, can also be used as a marker of apoptosis in culture and in tissue samples (Bressenot et al., 2009). PARP is a nuclear protein that binds to DNA strand breaks, acting as a signal for the enzymatic machinery that will repair the DNA break. In cells undergoing apoptosis, caspase-3 directly cleaves PARP into two smaller fragments, rendering it inactive (O'Brien et al., 2001). Immunostaining for activated-caspase-3 and PARP provide *in situ* detection of apoptosis, allowing the identification of individual apoptotic cells (Srinivasan et al., 1998). Western blotting provides an easy method of quantifying apoptosis in populations of cells (Janicke, 1998). Antibodies have been developed against a variety of targets in the apoptotic pathway, allowing flexibility in choosing whether you target an early or late apoptotic mediator. A limitation of this technique is the need to fix cells, leaving them no longer viable.

A variety of fluorogenic caspase substrates have also been developed to detect caspase activation as a marker of apoptosis (Liu et al., 1999; Cai et al., 2001; Wang et al., 2005). These substrates come in various forms with different tetrapeptide cleavage sequences allowing the detection of specific individual caspases. This technique involves incubating cell lysate with the fluorogenic substrate. The fluorogenic substrates shift their fluorescence emission maximum after cleavage by caspase-3 and are quantified using a fluorometer or fluorescence microtiter plate reader (Wang et al., 2005). This technique provides a quick and reliable method for quantifying caspase activation and apoptosis. This technique also offers the ability to target different caspases. A major limitation, however, stems from the fact that caspases exist as cytoplasmic enzymes. This requires lysis of the cells destroying the integrity of the sample.

1.3.5 Cytochrome C and Mitochondrial Detection Methods

The final method for apoptosis detection *in vitro* that will be discussed is targeted specifically at the mitochondrial or intrinsic apoptotic pathway. The major biochemical features of mitochondrial apoptosis are the opening of the MPT pore, loss of the mitochondrial transmembrane potential, and subsequent release of cytochrome c and other apoptotic proteins from the mitochondrial intermembrane space (Zimmermann and Green, 2001; Green and Kroemer, 2004). A variety of detection methods have been developed that target these molecular events. These assays are used to identify early apoptotic cells, as mitochondrial changes occur early on in the progression of apoptotic events (Fig. 2). Additionally, as these techniques are specific for the mitochondrial apoptotic pathway, they cannot detect apoptosis initiated through the external or death receptor pathway.

In healthy cells, cytochrome c is confined to the intermembrane space of the mitochondria. In cells undergoing apoptosis, cytochrome c is released from the intermembrane space to the cytosol where it becomes part of the apoptosome (Zou et al., 1999). Antibodies for cytochrome c provide a tool for the localization of cytochrome c through immunoblotting or immunostaining. Western blotting can compare cytochrome c

levels between cytosolic and mitochondrial fractions. Cytosolic fractions from cells undergoing apoptosis show an increase in cytochrome c staining compared to healthy cytosolic fractions (Bossy-Wetzel and Green, 2000). Additionally, subcellular distribution of cytochrome c can be analysed by immunostaining for cytochrome c. Healthy cells display punctate cyctochrome c staining within the mitochondria whereas apoptotic cells show more diffuse staining throughout the cytoplasm (Heiskanen et al., 1999). As with many of the assays discussed so far, cells are no longer left viable making this an end point for detection.

Another method for the detection of apoptosis based on mitochondrial changes involves tracking changes in the mitochondrial membrane potential. The opening of the MPT pore and loss of mitochondrial transmembrane potential is one of the earliest events in the intrinsic apoptotic pathway (Green and Kroemer, 2004). Cationic lipophilic dyes accumulate within the mitochondrial membrane as a result of the negative transmembrane potential produced during oxidative metabolism (Ehrenberg et al., 1988). The opening of the MPT pore and loss of transmembrane potential correlates to a loss of fluorescent dye due to the diminished capacity of the mitochondria to retain the probe (Johnson et al., 1981). The dye can be added to living cells and mitochondrial events can be imaged over time using FM or laser-scanning confocal microscopy. A major advantage of this technique is the ability to track mitochondrial changes associated with apoptosis in living cells in real time. A disadvantage of this technique is that disruption of the mitochondrial transmembrane potential can sometimes occur in necrosis, making this technique non-specific to apoptosis (Tsujimoto and Shimizu, 2007). Additionally, loss of membrane potential is a very early event in the apoptotic cascade, and its occurrence does not guarantee apoptosis will be carried out (Green and Kroemer, 2004).

1.4 Methods for Detecting Apoptosis *in Vivo*

1.4.1 Molecular Imaging

The development of molecular imaging techniques provides an opportunity to detect and image apoptosis *in vivo*. Molecular imaging can be defined as the non-invasive visualization of biochemical events at the cellular level in intact living organisms (Weissleder and Mahmood, 2001). In the past, *in vivo* imaging modalities have focused primarily on imaging gross anatomy. Disease progression and treatment outcomes were detected as structural changes and abnormalities using conventional techniques, such as X-ray, computed tomography (CT) imaging or magnetic resonance imaging (MRI) (Vernooij and Smits, 2012). More recently, advanced MRI techniques have probed brain function using functional MRI, structural connectivity using diffusion-weighted MRI, and metabolism using MR (magnetic resonance) spectroscopy (Lowe et al., 2000; Maheshwari et al., 2000; Hagmann et al., 2008; Bullmore et al., 2009; van den Heuvel and Hulshoff Pol, 2010). Now, with the emergence of new imaging contrast agents, it is possible to non-invasively image specific molecular targets in living, intact organisms. These targeted contrast agents can be used to visualize complex biochemical processes at the cellular level. Imaging can be performed in real-time, making it possible to follow molecular targets throughout the body and monitor changes in activity or consumption (James and Gambhir, 2012).

1.4.2 Molecular Imaging Modalities

There are a variety of imaging modalities that can be used for molecular imaging. The imaging modalities that are of specific interest in relation to this thesis include MRI and nuclear imaging techniques such as positron emission tomography (PET) and single-photon emission computed tomography (SPECT).

1.4.2.1 Magnetic Resonance Imaging

MRI has traditionally been used for structural imaging, and is capable of providing detailed anatomical information with excellent soft tissue contrast in the brain. This

imaging method uses radio frequency waves in the presence of a powerful magnetic field to obtain information about specific nuclei found within the body (Katti et al., 2011). Due to their high concentration in water molecules in the body, MRI images are primarily formed from hydrogen nuclei (^{1}H). The specific magnetic properties of these hydrogen nuclei are tissue specific and therefore can be used to produce detailed anatomical images (James and Gambhir, 2012).

The development of contrast agents (CA) has made it possible to use MRI for molecular imaging. CAs or imaging probes are exogenous substances that produce a bright signal, or a signal void in the MR image. They are usually injected into the body of the living organism and can be localized to particular tissues or areas within the body (James and Gambhir, 2012). The most commonly used MRI CAs are gadolinium (Gd) based and highlight vessels or regions of vascular permeability (Caravan et al., 1999). To provide meaningful biochemical information, contrast agents must be targeted toward specific biochemical events. For example, Gd-based CA can be fused to certain peptide sequences, antibodies, or targeting moieties (Park et al., 2008; Bort et al., 2014).

The major advantage associated with MRI is the extremely high spatial and temporal resolution. This makes it possible to track biomarkers inside the body and identify their exact position. The major limitation associated with this imaging technique is its low sensitivity, meaning a high concentration of CA must accumulate in the tissue before detection is possible (James and Gambhir, 2012).

1.4.2.2 Radionuclide Imaging

PET and SPECT imaging use unstable radionuclides to image biochemical events in living organisms. PET imaging utilizes unstable radioactive isotopes that decay via positron emission or beta decay. As the isotopes decay, they release gamma particles in opposite directions, which can be observed by detector pairs (coincidence counters) built in a ring surrounding the patient. The number of counts observed by each detector pair is used to compute a tomographic image (Basu et al., 2011). The most commonly used

radionuclide for PET imaging is fluorine-18 (^{18}F) (Alauddin, 2012). SPECT imaging uses the same fundamental principals to visualize physiological processes but different radioactive isotopes that emit gamma radiation. Gamma cameras are used to detect the radiation. The gamma cameras rotate around the patient to acquire multiple projections that are used to reconstruct tomographic images (Khalil et al., 2011). The most common radionuclides used for SPECT imaging are technetium-99m (^{99m}Tc), iodine-123 (^{123}I), and indium-111 (^{111}In) (Rudin and Weissleder, 2003).

Like MRI, in order to provide information on biochemical processes, the radiolabeled imaging agent must be targeted to specific molecular events. This can be achieved by labeling specific molecules, peptides, enzymes, or antibodies with radioactive isotopes. In the clinic, the most commonly used PET imaging agent is a radiolabelled analog of glucose, fluorodeoxyglucose (FDG). FDG is taken up by cells in living organisms and accumulates in cells with high metabolic activity. Generally, cancer cells have higher than normal glucose requirements and consequently take up more FDG than other tissues. This allows the visualization of tumors and cancer in living organisms using FDG and PET imaging (Gambhir, 2002).

The main advantage associated with radionuclide imaging is its excellent sensitivity. PET and SPECT imaging are much more sensitive than MRI, allowing for the use of nanomolar concentrations of imaging agent. Unfortunately, what PET and SPECT imaging gain in sensitivity they lose in spatial resolution (James and Gambhir, 2012).

1.4.3 Molecular Imaging of Apoptosis

The proteolytic cascade and biochemical hallmarks associated with apoptosis provide a number of potential targets for the molecular imaging of apoptosis. Despite the diverse array of targets, an adequate method ready for clinical use has yet to be developed for the *in vivo* detection of apoptosis. This section will outline some of the existing methods for detecting apoptosis in living organisms and discuss their shortcomings.

1.4.3.1 Radiolabelled Annexin V

To date, the most successful method for imaging apoptosis has been the use of radiolabelled Annexin V (Tait, 2008). This is a direct extension of the *in vitro* imaging technique that uses fluorescently labeled Annexin V to bind to PS on the outer leaflet of apoptotic cells.

In 1998, Blankenberg et al. were the first group to demonstrate the ability to detect apoptosis *in vivo* using radiolabeled Annexin V. Using ^{99m}Tc-labelled Annexin V they demonstrated the ability to detect apoptosis in three different mouse models of apoptosis. Imaging showed a two- to six-fold increase in the uptake of radiolabelled Annexin V at the sites of apoptosis in all three models. The most impressive results were seen in cyclophosphamide treated murine B-cell lymphomas. Twenty hours after the injection of radiolabelled Annexin V cyclophosphamide treated tumours displayed 3-4 times higher uptake than controls (Blankenberg et al., 1998).

In 2002, Belhocine et al. conducted one of the first human studies using radiolabelled Annexin V to predict tumour response to chemotherapy in individuals with cancer. Many chemotherapeutic drugs work by inducing apoptosis in target tumours; however, some tumours can show greater resistance to chemotherapy than others. In this study, the authors predicted that ^{99m}Tc-labelled Annexin V uptake in tumors, indicative of apoptosis, would correlate to tumor response to treatment. Fifteen patients presenting with either lung cancer, lymphoma or breast cancer were administered ^{99m}Tc-labelled Annexin V before and within 3 days of receiving their first dose of chemotherapy. FDG and PET scans were used to evaluate tumor response 3 months after chemotherapy treatment. For all individuals in the study, no agent uptake was observed in the tumor during the first scan before receiving chemotherapy. Following chemotherapy, the 7 patients who showed ^{99m}Tc labeled Annexin V uptake at the tumor site, had complete (n = 4) or partial response (n = 3). In contrast, 6 of the 8 patients who did not show significant Annexin V uptake had progressive disease. This study demonstrated the ability of ^{99m}Tc-labelled Annexin V to localize to tumor sites following chemotherapy

and suggests its ability to predict tumor outcome in response to treatment. This study also demonstrated the safety of using ^{99m}Tc-labelled Annexin V in humans. While this study showed some success, the target-to-background ratio of the agent was low. The liver and kidneys demonstrated much higher uptake of ^{99m}Tc-labelled Annexin V compared to the uptake seen in the tumor (Belhocine et al., 2002).

Radiolabelled Annexin V has also been used to image stroke in rodents and humans (Blankenberg et al., 2006; Lorberboym et al., 2006). Lorberboym *et al.* evaluated the potential of radiolabelled Annexin V to image ischemic injury in human patients with acute cerebral stroke. Compared to control patients, eight out of twelve stroke patients displayed abnormal uptake of ^{99m}Tc-labelled Annexin V in the infarct regions. The integrity of the BBB was also evaluated using ^{99m}Tc labeled diethylene-triamine-pentaacetate (DTPA). All of the patients who underwent DTPA imaging showed breakdown of the BBB (Lorberboym et al., 2006). Although this study demonstrated the ability of ^{99m}Tc labeled Annexin V to detect ischemic injury in patients with acute cerebral stroke, it raised some red flags for the use of this imaging agent in the CNS. First, the ability of radiolabelled Annexin V to cross the BBB is questioned in this study. The patients who underwent DTPA imaging all demonstrated breakdown of the BBB. Without breakdown of the BBB, labeled Annexin V may not be capable of entering the CNS. This limits the ability of this agent to image cell death in situations where the BBB is intact. Additionally, Annexin V will bind to both apoptotic and necrotic cells and is unable to differentiate the two. While this is useful for detecting stroke where both types of cell death occur, it does not offer the potential to image purely apoptotic cell death. The ability to distinguish apoptosis from necrosis *in vivo* could be very valuable in understanding the role that programmed cell death plays in a variety of pathological conditions.

1.4.3.2 Labeled Caspase-3 Substrates

Although caspase imaging probes have great potential, there has been limited work done in animals and no human studies. Bullok *et al*. reported the ability of a caspase-activatable probe to detect parasite-induced apoptosis in human colon xenograft and liver abscess mouse models. Their caspase-3 probe consisted of a cell penetrating peptide conjugated to a caspase-3 cleavage site that was flanked by a fluorophore-quencher pair. Cleavage by caspase-3 resulted in release of the quencher and emergence of fluorescent signal (Bullok et al., 2007). Although their caspase-activatable probe was able to image apoptosis in mice, fluorescence imaging is not possible in deeper tissues, limiting the clinical application of this probe.

1.5 Rationale and Hypothesis

Although important in normal development, apoptosis can contribute to neurodegeneration and has been associated with a number of neurodegenerative disorders, including AD, PD, and HD (Mattson, 2000). As Canada's population ages and the incidence of neurodegenerative disorders rapidly increases, there is a critical need to improve the early detection and diagnosis of neurodegenerative disease (Mayeux, 2003). A contrast agent capable of detecting apoptosis *in vivo* may prove to be very useful in the early diagnosis of neurodegenerative disease. The ability to detect neurodegeneration before the onset of symptoms would significantly impact treatment therapies and help alleviate the economic burden of the disease.

We have developed a novel contrast agent for the detection of apoptosis *in vivo*. The contrast agent is targeted toward the detection of caspase-3, the key enzymatic mediator of apoptosis. The agent incorporates both a caged lanthanide metal ion for MRI detection and Oregon Green for optical/fluorescent detection. This imaging agent is coupled to a cell-penetrating peptide derived from the Tat sequence of the HIV virus, by a peptide backbone containing a caspase-3 cleavage site (Fig. 3). The cell-penetrating peptide

allows the contrast agent to cross cell membranes and the blood brain barrier in both directions. In cells undergoing apoptosis, activated caspase-3 will cleave the agent at the caspase-3 cleavage site, releasing the cell-penetrating peptide and trapping the imaging probes inside the cell. One single activated-caspase-3 protein can cleave multiple contrast agent molecules, leading to the accumulation of the contrast agent inside the cell or blood brain barrier, and resulting in the amplification of observed signal.

We hypothesize that a contrast agent targeted toward the detection of caspase-3 can be used to image apoptosis *in vivo*. The objective of this project was to test the ability of the contrast agent to label apoptotic cells in culture and explore its potential to detect apoptosis *in vivo*.

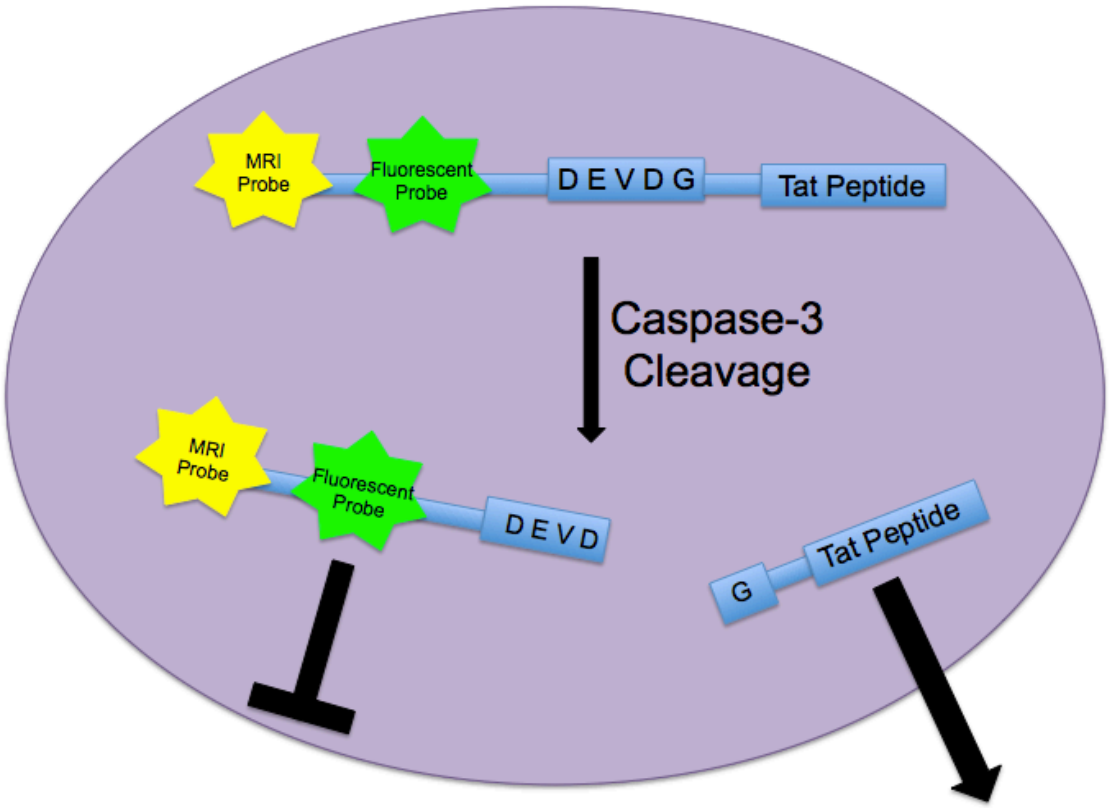

Figure 3. Schematic representation of our contrast agent. Our contrast agent consists of a dual magnetic resonance imaging/fluorescent probe coupled to a cell penetrating

peptide (CPP) sequence by a peptide backbone containing a caspase-3 cleavage site. In cells undergoing apoptosis, activated caspase-3 will cleave the agent at the caspase-3 cleavage site, releasing the CPP and trapping the imaging probes inside the cell.

Chapter 2

2 Methods

All animal studies were conducted in accordance with the guidelines of the Subcommittee on Animal Care at the University of Western Ontario, and conformed to the Canadian Council on Animal Care guide for the care and use of laboratory animals.

2.1 Contrast Agent Synthesis

The contrast agent, Gd^{3+}-DOTA-Cas-3, was synthesized and characterized by high resolution electron spray ionization mass spectrometry in a similar manner as described by Suchy *et al*. To synthesize Gd^{3+}-DOTA-Cas-3 the peptide sequence for the caspase-3 cleavage site (DEVD) was used instead of the peptide sequence for the cathepsin-D cleavage site. Purified Gd^{3+}-DOTA-Cas-3 was dissolved in water (1mM stock), aliquoted, and stored at -20°C.

2.2 Fluorescence Microscopy

All images were acquired using a Zeiss Axiovert 100 inverted fluorescence microscope and AxioCam HRm camera (Carl Zeiss, Germany). A Zeiss 40× 0.6 numerical aperture dry lens was used to acquire images for experiments analyzing contrast agent uptake in individual cells and to characterize apoptosis. A Zeiss 20× 0.5 numerical aperture dry lens was used to acquire images for experiments analyzing contrast agent uptake in populations of cells. A Zeiss 10× 0.3 numerical aperture dry lens was used to acquire images of tyrosine hydroxylase staining in the substantia nigra (SN). A Zeiss 63× 1.4 numerical aperture oil immersion lens was used to image contrast agent uptake in the SN.

The contrast agent was visualized using a 450-490 nm excitation band pass filter set and 515-565 nm emission band pass filter set. Hoechst 33342 was visualized using a 365/12 nm excitation band pass filter set and 397 nm long pass filter set. PI, Alexafluor 546 secondary antibody, and Alexa Fluor 594 TUNEL stain were imaged using a 546/12 nm

excitation band pass filter set and 575-640 nm emission band pass filter set. DAB staining was visualized using transmitted light.

2.3 N2A Cell Culture

The neuro-2A (N2A) mouse neuroblastoma cell line was purchased from ATCC (Manassas, Virginia). Cells were maintained in minimal essential media (MEM; Invitrogen, Grand Island, NY) supplemented with 10% heat-inactivated fetal bovine serum (Hyclone, Logan, UT) and 100 μg/mL penicillin-streptomycin (Invitrogen, Grand Island, NY). Cells were seeded in 4-well plates (Thermo Scientific, Mississauga, ON) at a concentration of 1×10^5 N2A cells per well. Cells were grown at 37°C in an atmosphere of 5% CO_2. Cells were treated with camptothecin (CPT), 1-methyl-4-phenylpyridinium (MPP^+), tunicamycin and staurosporine 2-3 days after plating (all from Sigma Aldrich, Oakville, ON). Drugs were diluted in culture media immediately before adding to cultures. Stock solutions of CPT, tunicamycin and staurosporine were stored at -20°C and fresh MPP^+ stock was made before each addition to cell media. Control cells were incubated in regular culture medium without the addition of a pro-apoptotic stimulus. Following treatment, cells were fixed and stained with an antibody against cleaved caspase-3 (1:400 dilution; Cell Signaling, Beverly, MA) and counterstained with DAPI (4',6-Diamidino-2-Phenylindole; Invitrogen, Grand Island, NY). The primary antibody was detected using an Alexafluor 546 secondary antibody (Invitrogen, Grand Island, NY).

2.4 Primary Neuronal Culture

Cortical neurons were dissociated and prepared from E15.5 mouse embryos as previously described by Fortin *et al*.. Cells were plated onto poly-L-ornithine-coated (Sigma Aldrich, Oakville, ON) 4-well plates and 35 mm glass-bottomed confocal dishes (Thermo Scientific, Mississauga, ON) at a density of 2.5×10^5 cells per well and 1×10^6 cells per dish, respectively. Cells were grown in serum-free Neurobasal medium supplemented with B27, N2, 2 mM GlutaMax (l-glutamine) and 50 μg/mL penicillin-streptomycin

(Invitrogen, Grand Island, NY) at 37°C in 5% CO_2. After 3 days, one-half of the media was removed and replaced with fresh culture media. Cells were used for experiments on days 4-7 of culture.

To determine the proportion of cells in primary culture that were neurons, cells were fixed and stained with an antibody against NeuN (1:200; Abcam, Toronto, ON) and counterstained with DAPI (Invitrogen, Grand Island, NY). The primary antibody was detected using an Alexafluor 546 secondary antibody (Invitrogen, Grand Island, NY). The proportion of NeuN positive cells as a percentage of total cell number was determined.

2.5 Induction of Apoptosis in Primary Cortical Neurons

Cortical neurons were seeded in confocal dishes and treated with 10 μM CPT (Sigma Aldrich, Oakville, ON) for 24 hours to induce apoptosis. Control neurons remained in regular culture medium for 24 hours. Following treatment, cells were fixed and stained with antibodies against cleaved caspase-3 (1:400 dilution; Cell Signaling, Beverly, MA) and counterstained with DAPI (Invitrogen, Grand Island, NY). The primary antibody was detected using an Alexafluor 546 secondary antibody (Invitrogen, Grand Island NY).

2.6 Optimization of Contrast Agent Concentration and Exposure Time

Cortical neurons seeded in 4-well plates were treated with 10 μM CPT (Sigma Aldrich, Oakville, ON) for 24 hours to induce apoptosis. Cells were then exposed to different concentrations of the contrast agent for varying lengths of time. Before imaging, cells were washed 3 times with warm Hanks buffered saline solution (HBSS; Invitrogen, Grand Island, NY).

2.7 Contrast Agent Toxicity

To evaluate the toxicity of the contrast agent, neurons were exposed to the working concentration of the contrast agent (10 μM) for increasing lengths of time. Primary

neurons seeded in 4-well plates were incubated with 10 μM of the contrast agent for 4, 8, or 24 hours. Control cells were incubated in regular culture media without the addition of contrast agent. At the end of the incubation period, Hoechst 33342 (1.62 μM; Sigma Aldrich, Oakville, ON) and PI (500 nM; Sigma Aldrich, Oakville, ON) were added directly to the culture medium and cells were not washed before imaging. Cell viability was assessed using Image J software to determine the proportion of nuclei that exhibited PI negative staining. A minimum of 800 cells was scored for each treatment and the data represent the mean and standard error from three different experiments.

2.8 Cellular Uptake and Retention of Contrast Agent in Apoptotic Neurons

Primary neurons were seeded in confocal dishes and treated with either CPT or MPP^+ (both from Sigma Aldrich, Oakville, ON) at 10 μM concentration for 24 h. Stock solutions of CPT and MPP^+ were diluted in culture media immediately before adding to cultures. CPT stock was stored at -20°C and fresh MPP^+ stock was made before each addition to cell media. Control cells remained in regular culture medium for 24 hours. For inhibitor studies, 50 μM of the caspase-3 inhibitor Z-DEVD-FMK (EMD Millipore, Etobicoke, ON) was added to culture media 1 hour prior to treatment with either CPT or MPP^+.

Neurons were incubated with 10 μM contrast agent for 4 h prior to imaging (20 h after adding CPT or MPP^+). The contrast agent was diluted in culture media before adding to cultures. Before imaging, neurons were washed three times with warm HBSS (Invitrogen, Grand Island, NY) to remove free-floating contrast agent and reduce background. Cells were subsequently stained with Hoechst 33342 (1.62 μM; Sigma Aldrich, Oakville, ON) and PI (500 nM; Sigma Aldrich, Oakville, ON) and imaged live.

To evaluate the ability of our contrast agent to selectively label apoptotic cells, confocal dishes were treated with 10 μM of CPT for 24 h to generate a combination of apoptotic, living and dead cells. Images were taken using the 40× objective lens and living,

apoptotic and dead cells were defined by examining nuclear morphology in Hoechst 33342 and PI stained cells. Cells exhibiting pyknotic and/or fragmented nuclei with negative PI staining were characterized as apoptotic. Cells displaying healthy diffuse nuclei with negative PI staining were characterized as healthy. Cells with positive PI staining (regardless of nuclear morphology) were considered dead. The proportion of cells retaining contrast agent within each population of apoptotic, living or dead cells was quantified by analyzing the number of cells in each population that retained the contrast agent and appeared bright green. A minimum of 200 cells was characterized as apoptotic, living or dead in each experiment and assessed for contrast agent uptake. The data represent the mean and standard error of the percentage of neurons retaining the contrast agent within each population from four independent experiments.

To compare contrast agent uptake between control neurons, neurons induced to undergo apoptosis and neurons induced to undergo apoptosis in the presence of a caspase-3 inhibitor, images were acquired using the 20× objective lens. Image J was used to count the total number of nuclei in each image field. The proportion of cells that retained the contrast agent was quantified by counting the number of cells that appeared bright green and dividing by the total number of nuclei. A minimum of 500 cells was counted for each treatment and the data represent the mean and standard error from three different experiments. To evaluate apoptosis in each condition, images were acquired using the 40× objective lens. The proportion of nuclei displaying negative PI staining and typical apoptotic nuclear morphology was scored. A minimum of 160 cells was evaluated for each treatment and the data represent the mean and standard error from three different experiments.

2.9 Cellular Uptake and Retention of Contrast Agent in Necrotic Neurons

For the induction of necrosis in primary culture, cells were treated with 500 μM of N-methyl-D-aspartate (NMDA; Sigma Aldrich, Oakville, ON) for 6 h. Two hours after the addition of NMDA, cells were incubated with 10 μM of the contrast agent for 4 hours.

Immediately before imaging, cells were washed three times with warm HBSS (Invitrogen, Grand Island, NY) and subsequently stained with Hoechst 33342 (1.62 μM; Sigma Aldrich, Oakville, ON) and PI (500 nM; Sigma Aldrich, Oakville, ON). Image J was used to count the total number of nuclei and PI positive nuclei in each image field. The proportion of cells that retained the contrast agent was quantified by counting the number of cells that appeared bright green and dividing by the total number of nuclei. A minimum of 650 cells was counted for each treatment and the data represent the mean and standard error from four different experiments.

2.10 1-Methyl-4-Phenyl-1,2,3,6-Tetrahydropyridine Injections

Ten to twelve week old male C57Bl/6 mice weighing 25-30 g were used for the MPTP injections (Charles River, Wilmington, MA). Mice were habituated for 7 days prior to starting injections. Animals were housed 2-4 per cage in a temperature-controlled room in a 12 h light/12 h dark cycle with free access to food and water.

MPTP-HCl (Sigma Aldrich, Oakville, ON) was dissolved in sterile 0.9% NaCl. Experimental mice received intraperitoneal (IP) injections of 30 mg/kg MPTP once per day for five consecutive days. Control mice were injected IP with 0.9% NaCl. Three days after the final MPTP injection mice were injected with the contrast agent.

Mice were anesthetized with 4% isofluorane and oxygen. A tail-vein catheter was established and a saline flush was performed to ensure that the catheter was accurately placed. Mice were injected intraveneously with 80 μL of 1 mM contrast agent. One mouse from each the MPTP-treated and control group was not injected with contrast agent to allow for comparison of background auto-fluorescence.

Following contrast agent injection, one mouse from each the MPTP-treated and control group was sacrificed at 1 and 2 hours to analyze cell death and contrast agent distribution throughout the brain. The mice were deeply anaesthetized with a cocktail of ketamine and xylazine (0.1ml/10g) and perfused via the left ventricle with 0.1 M ice-cold phosphate-buffered saline (PBS; Invitrogen, Grand Island, NY) followed by 4% ice-cold

paraformaldehyde (PFA; Sigma Aldrich, Oakville, ON). The brains were dissected and fixed by immersion in PBS/4% paraformaldehyde for 24 h at 4°C.

2.11 Histological Analysis of MPTP-Treated and Control Mice

Following fixation, mouse brains were paraffin embedded. A Microm HM 335 E Microtome (Thermo Scientific, Mississauga, ON) was used to coronally cut through the SN at a thickness of 5 μM. Sections were mounted on glass slides and stained with an antibody against tyrosine hydroxylase (1:500; Abcam, Toronto, ON). Primary antibody was detected with a secondary antibody conjugated to horseradish peroxidase and developed with a diaminobenzidine (DAB) stain using Vectastain ABC kit (Vectorlabs). To detect DNA fragmentation, slides were stained with the Click-iT Alexa Fluor 594 TUNEL assay (Invitrogen; Grand Island, NY) according to manufacturers instructions. To analyze contrast agent distribution, slides were counterstained with hematoxylin.

2.12 Statistical Analysis

Data are presented as the mean ± SEM with n values representing the number of independent cell cultures or individual animals. For cellular experiments, each n value was obtained by averaging at least 8 images taken from random fields in each experiment. For animal experiments, each n value was obtained by imaging at least 4 brain sections from one mouse. Image J was used to analyze cell counts. GraphPad Prism 6 was used to analyze data, using unpaired student's t-test or one-way ANOVA followed by Tukey's post hoc to determine statistical significance.

Chapter 3

3 Results

3.1 N2A Cells Do Not Easily Undergo Chemical-Induced Apoptosis

To evaluate the ability of our contrast agent to label apoptotic cells we needed a method for inducing apoptotic cell death in culture. N2A cells are a mouse neuroblastoma cell line that demonstrate neuronal morphology (Tremblay et al., 2010). It has previously been shown that it is possible to induce apoptosis in N2A cells using a variety pro-apoptotic drugs (Sheehan et al., 1997; Ito et al., 2004; Li et al., 2007; Galehdar et al., 2010; Wang et al., 2010). Therefore, we treated N2A cells with different pro-apoptotic drugs and evaluated their ability to induce apoptosis. After treatment with the drugs, cells were fixed and stained for activated caspase-3 and counterstained with 4',6-Diamidino-2-Phenylindole (DAPI). Apoptosis was assessed based on nuclear morphology and caspase-3 activation.

In our study, cells treated with previously suggested (Sheehan et al., 1997; Ito et al., 2004; Li et al., 2007; Galehdar et al., 2010; Wang et al., 2010) concentrations of camptothecin (CPT; 10 μM), 1-methyl-4-phenylpyridinium (MPP^+; 10 μM), staurosporine (10 μM) or tunicamycin (2 μg/mL) did not display apoptotic nuclear morphology (pyknotic or fragmented nuclei) or caspase-3 activation (Fig. 4). When the concentration of drugs was increased by a factor of 5 (CPT, 50 μM; MPP^+, 50 μM; staurosporine, 50 μM; tunicamycin 10 μg/mL) apoptotic nuclear morphology and caspase-3 activation were still not observed (Fig. 4). In the event that 24 hours was not long enough for the induction of apoptosis, the treatment period with the drugs was extended to 36 and 48 hours. Even with an extended incubation period with the pro-apoptotic drugs there was almost no evidence of apoptosis (data not shown).

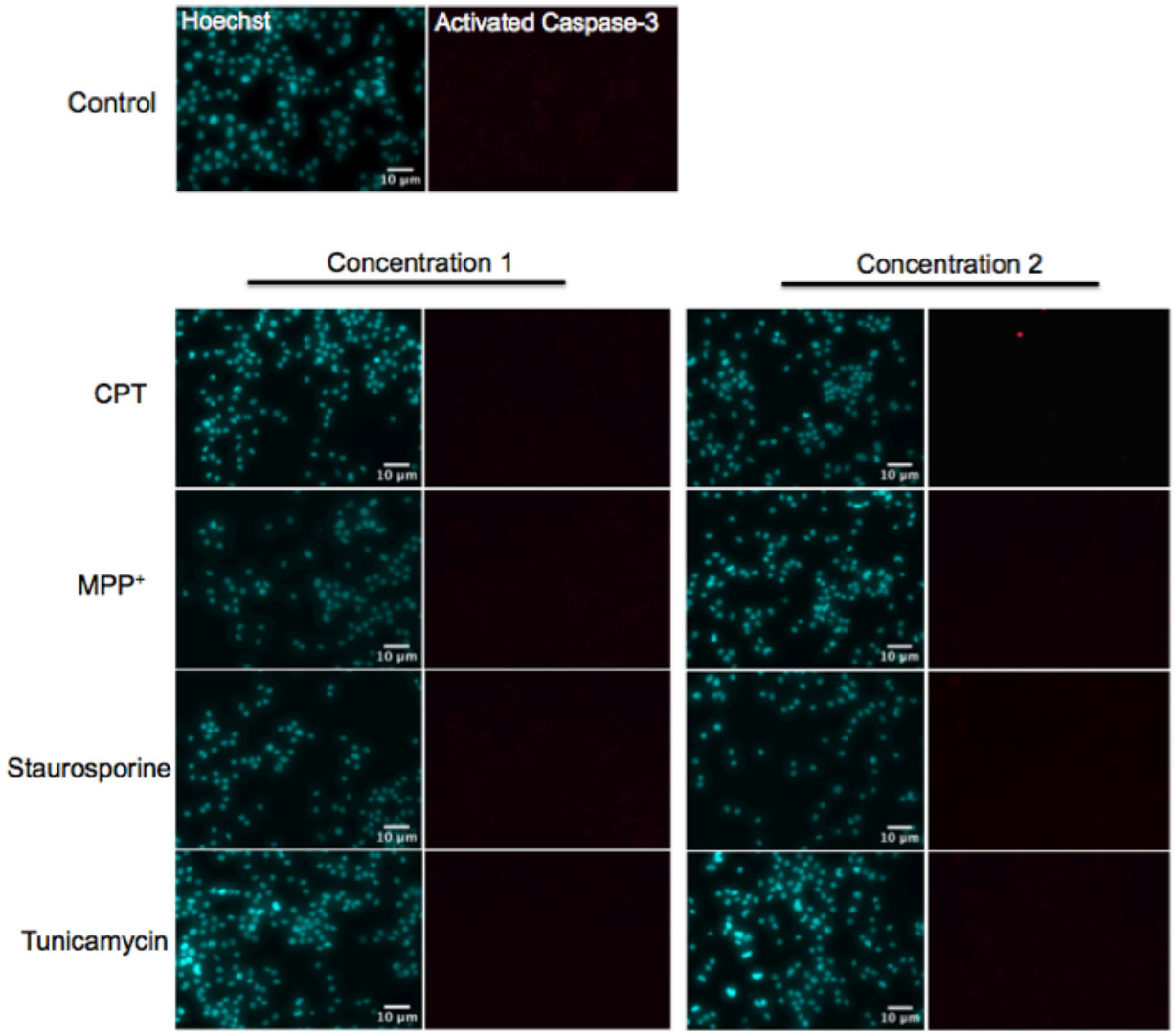

Figure 4. N2A cells do not display apoptotic nuclear morphology or caspase-3 activation in response to pro-apoptotic drugs. N2A cells were treated with CPT (10 µM, 50 µM), MPP^+ (10 µM, 50 µM), staurosporine (10 µM, 50 µM), or tunicamycin (2 µg/mL, 10 µg/mL) for 24 hours. Control neurons were left untreated and remained in regular culture medium. Cells were fixed and stained for activated caspase-3 and counterstained with DAPI. Similar to control cells, treated N2A cells did not display pyknotic or fragmented nuclei characteristic of apoptosis. In addition, treated N2A cells did not display caspase-3 activation.

3.2 Mouse Primary Cortical Neurons Undergo Chemical-Induced Apoptosis

In the previous study, the N2A neuroblastoma cell line displayed significant resistance to regular apoptotic stimuli. In order to develop a model for inducing apoptosis in culture we turned to mouse primary cortical neurons. Primary neurons are known to be more sensitive to cell death and apoptotic stimuli than cell lines, making them a better candidate to model apoptosis. Figure 5 displays a representative image depicting NeuN immunostaining in the primary neuronal culture. Immunostaining for NeuN demonstrated that > 95% of the nuclei counted in the primary culture stained positive for NeuN, confirming that the majority of cells in primary culture were neurons.

When treated with 10 μM CPT for 24 hours, mouse primary cortical neurons appeared to readily undergo apoptosis. Immunocytochemistry with an antibody against activated caspase-3 demonstrated widespread caspase-3 activation throughout CPT-treated neurons. The nuclear stain DAPI revealed many neurons with pyknotic and fragmented nuclei, typical of apoptosis (Fig 6A). This was in contrast to control neurons that displayed healthy, diffuse nuclear staining and minimal caspase-3 activation (Fig. 6A). Additionally, high power images (40×) revealed that caspase-3 activation was specific to neurons that displayed either pyknotic or fragmented nuclei (Fig. 6B). This confirms our ability to assess apoptosis and caspase-3 activation based on nuclear morphology.

3.3 Contrast Agent Optimization

The purpose of the next experiment was to determine the optimal contrast agent concentration and exposure time to detect apoptosis in culture. We have demonstrated the ability to induce apoptosis in primary neurons by treating them with 10 μM camptothecin for 24 hours. Therefore, we induced apoptosis under the same conditions and compared contrast agent uptake and retention in neurons exposed to varying concentrations of the contrast agent for different lengths of time. We compared uptake and retention in neurons exposed to 5, 10, 25, and 50 μM of the contrast agent for 1, 2 and 4 hours.

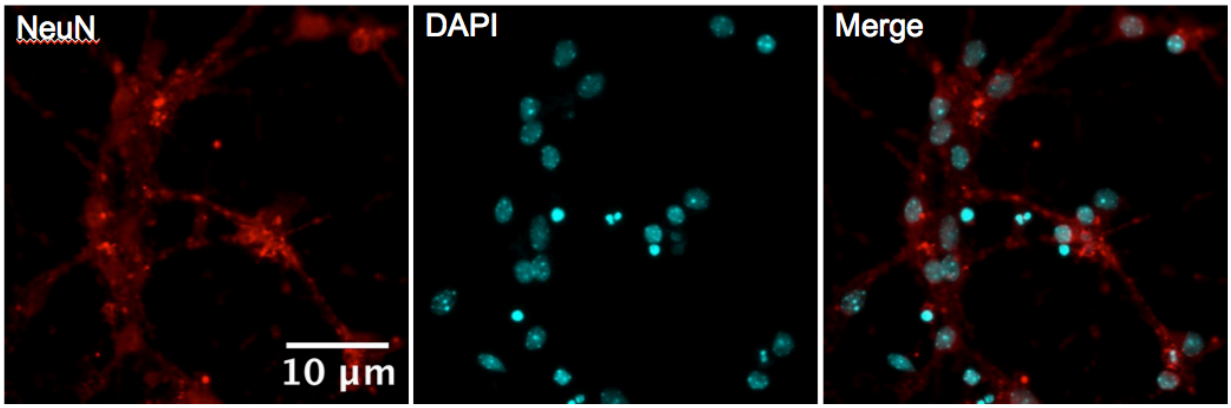

Figure 5. NeuN immunostaining in mouse primary cortical neuron culture. Primary cortical neurons were fixed and immunostained for NeuN and counterstained with DAPI. More than 95% of nuclei stained positive for NeuN, demonstrating that the majority of cells in culture were neurons.

Figure 7 displays representative images of contrast agent uptake at each concentration and at each length of time. All images were taken using the same settings and intensity. Agent uptake appeared to occur in a concentration dependent manner and increasing the incubation period with the contrast agent increased the number of cells that retained the agent. Increasing the contrast agent concentration beyond 10 µM greatly increased the amount of background fluorescence. For this reason it was determined that exposing neurons to 10 µM of the contrast agent for 4 hours were the optimal conditions for detecting apoptosis.

3.4 Cell Viability Studies

Toxicity is a major concern when developing contrast agents for future work with animals and humans. For a preliminary assessment of the toxicity of our contrast agent, primary cortical neurons in culture were exposed to the working concentration of our contrast agent (10 µM) for varying lengths of time. Neurons were stained with Hoechst 33342 and propidium iodide (PI) to determine the proportion of viable and dead cells. Negative PI staining was used to identify the nuclei of living cells and positive PI

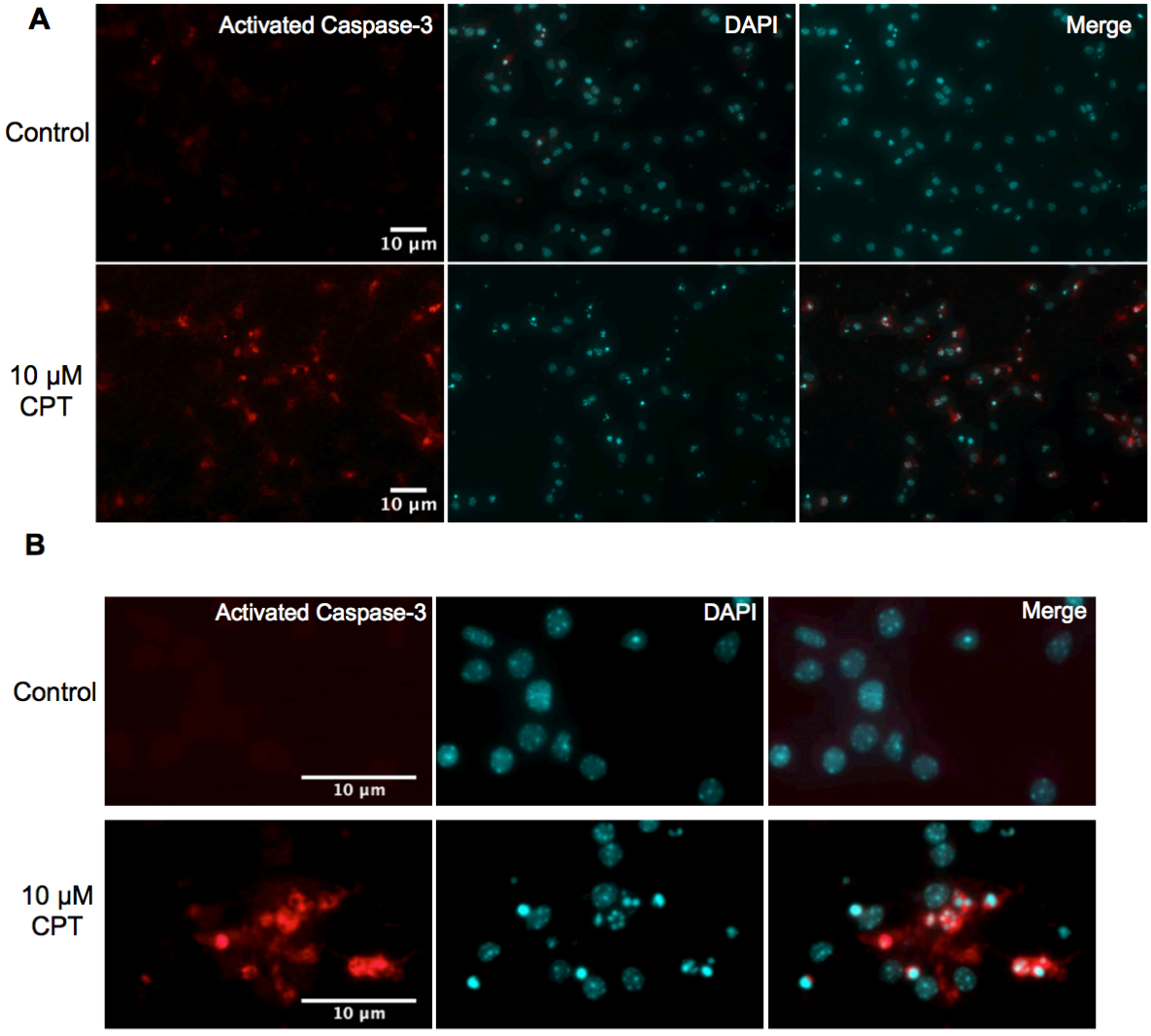

Figure 6. Mouse primary cortical neurons undergo apoptosis and caspase-3 activation in response to camptothecin treatment. Primary cortical neurons were treated with 10 µM CPT for 24 hours. Control neurons remained untreated. Neurons were fixed and immunostained for activated caspase-3 and counterstained with DAPI. A. Neurons treated with CPT demonstrate caspase-3 activation and display pyknotic and fragmented nuclei characteristic of apoptosis. B. High power image demonstrating that neurons with pyknotic or fragmented nuclei demonstrate caspase-3 activation.

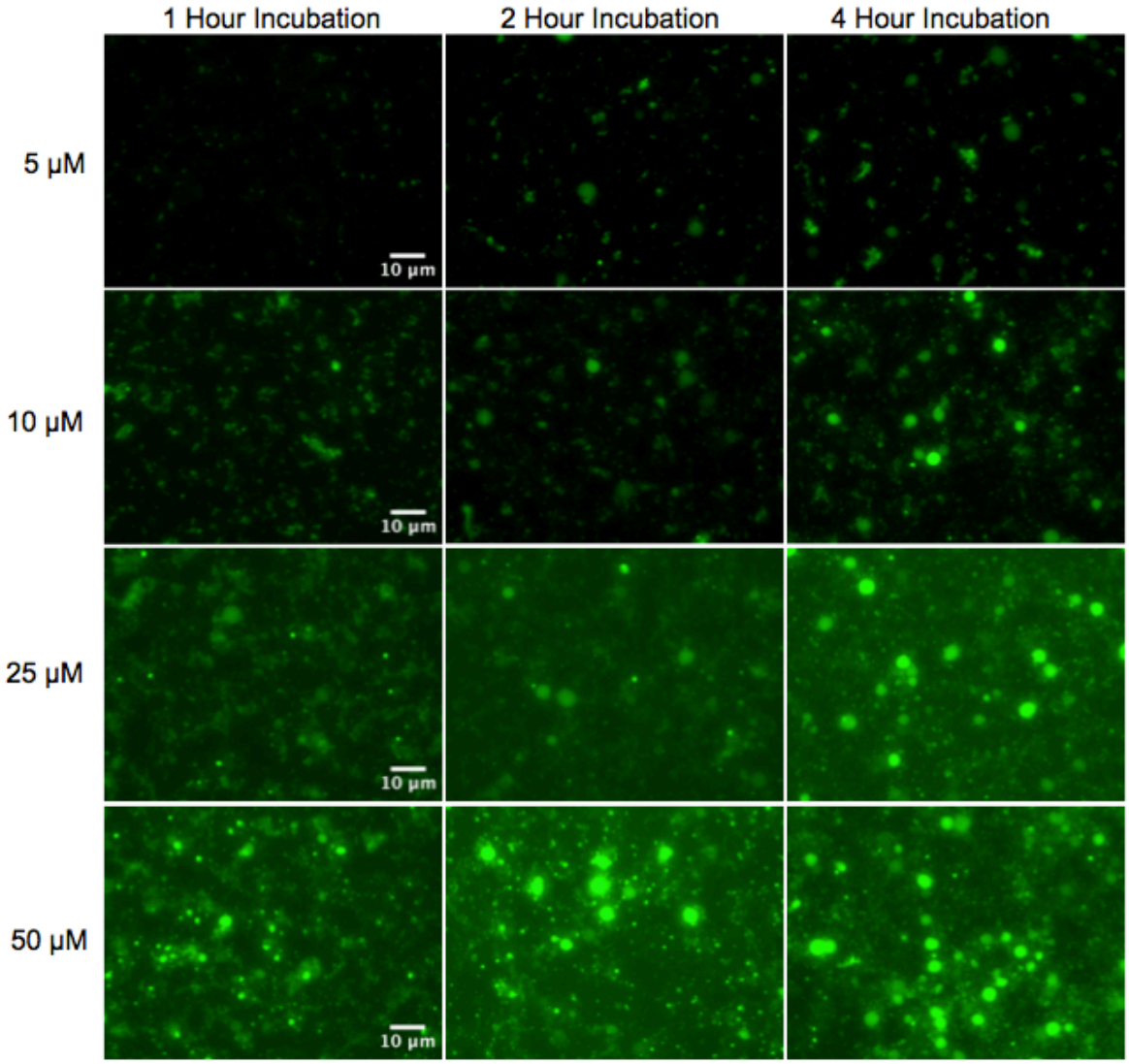

Figure 7. Optimization of contrast agent concentration and incubation time. Primary cortical neurons were treated with 10 µM CPT for 24 hours to induce apoptosis. Neurons were then incubated with the indicated concentration of contrast agent for the indicated amount of time. Cells were then washed and imaged live using a fluorescent microscope. All images were acquired at the same settings and intensity. Increasing the exposure time to the contrast agent increased the number of cells that retained the contrast agent. Cells incubated with 10 µM of contrast agent for 4 hours demonstrated adequate contrast agent uptake with reduced background.

staining was used to identify the nuclei of dead cells.

Figure 8 displays that at 4, 8, and 24 hours, 70 ± 5, 75 ± 5, and 70 ± 3 % of neurons, respectively, were viable. Control neurons incubated in regular culture medium for 24 hours were 74 ± 4 % viable. One-way ANOVA revealed that there were no significant differences between the percentage of neurons surviving in control conditions and neurons exposed to the contrast agent for up to 24 hours.

3.5 Evaluation of Contrast Agent Uptake in Individual Neurons

The primary goal of this study was to evaluate the ability of our contrast agent to label apoptotic cells. By treating neurons with CPT for 24 hours we were able to compare contrast agent uptake and retention on a cell-by-cell basis between living, apoptotic and dead cells. This allowed us to evaluate the ability of our contrast agent to selectively label apoptotic cells over living or dead cells.

Treatment of primary neurons with CPT for 24 hours yields a combination of living, apoptotic and dead cells. Neurons are classified as dead when they have lost their membrane integrity and stain positive for PI. Apoptotic cells are PI negative (still maintaining membrane integrity) and exhibit pyknotic or fragmented nuclei characteristic of apoptosis. Living cells are also PI negative but display healthy nuclear morphology.

Primary neurons were treated with 10 μM CPT for 24 hours. During the last 4 hours of treatment 10 μM of contrast agent was added to the neuron medium. At the end of the incubation period the neurons were washed to remove free-floating contrast agent and stained with Hoechst 33342 and PI. Cells were imaged live using fluorescence microscopy. Based on the criteria described above, cells were characterized as living, apoptotic or dead. The proportion of cells that retained the contrast agent in each

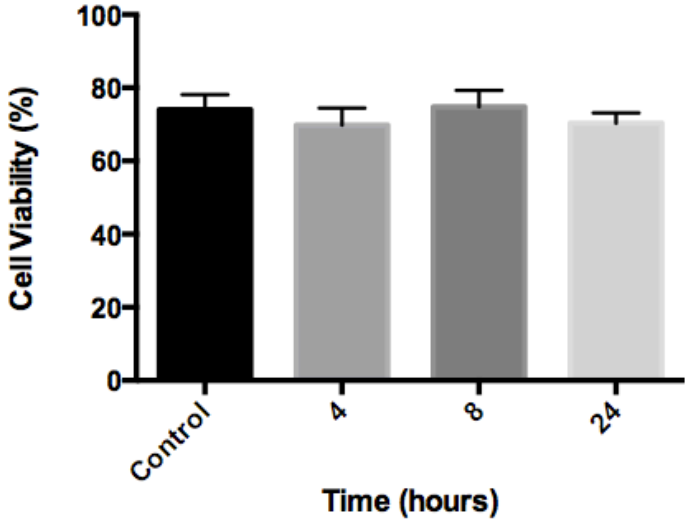

Figure 8. Exposure to contrast agent for up to 24 hours does not affect cell viability. Primary cortical neurons were incubated with 10 μM contrast agent for the indicated amount of time. Control neurons were left in regular culture medium for 24 hours. Cells were imaged live using fluorescence microscopy and stained with Hoechst 33342 and propidium iodide (PI). The proportion of PI negative cells was used to assess cell viability (n=3). There were no statistically significant differences in cell viability between any of the time points. Error bars represent standard error of the mean.

population was quantified by counting the number of cells that demonstrated bright green fluorescent signal within each population (Fig. 9A).

In this study, over 500 cells from 4 independent experiments were characterized as apoptotic and 55 ± 5 % of them retained the contrast agent. In contrast, we counted over 200 living and 200 dead cells, of which 2 ± 1 % of the living cells retained the contrast agent and 17 ± 3 % of the dead cells retained the contrast agent. One-way ANOVA followed by Tukey's post-hoc demonstrated that a significantly greater proportion of apoptotic cells retained the contrast agent in comparison to healthy or dead cells (Fig. 9B; $p < 0.0001$). These results indicate that our contrast agent is capable of selectively labeling and detecting apoptotic cells in culture.

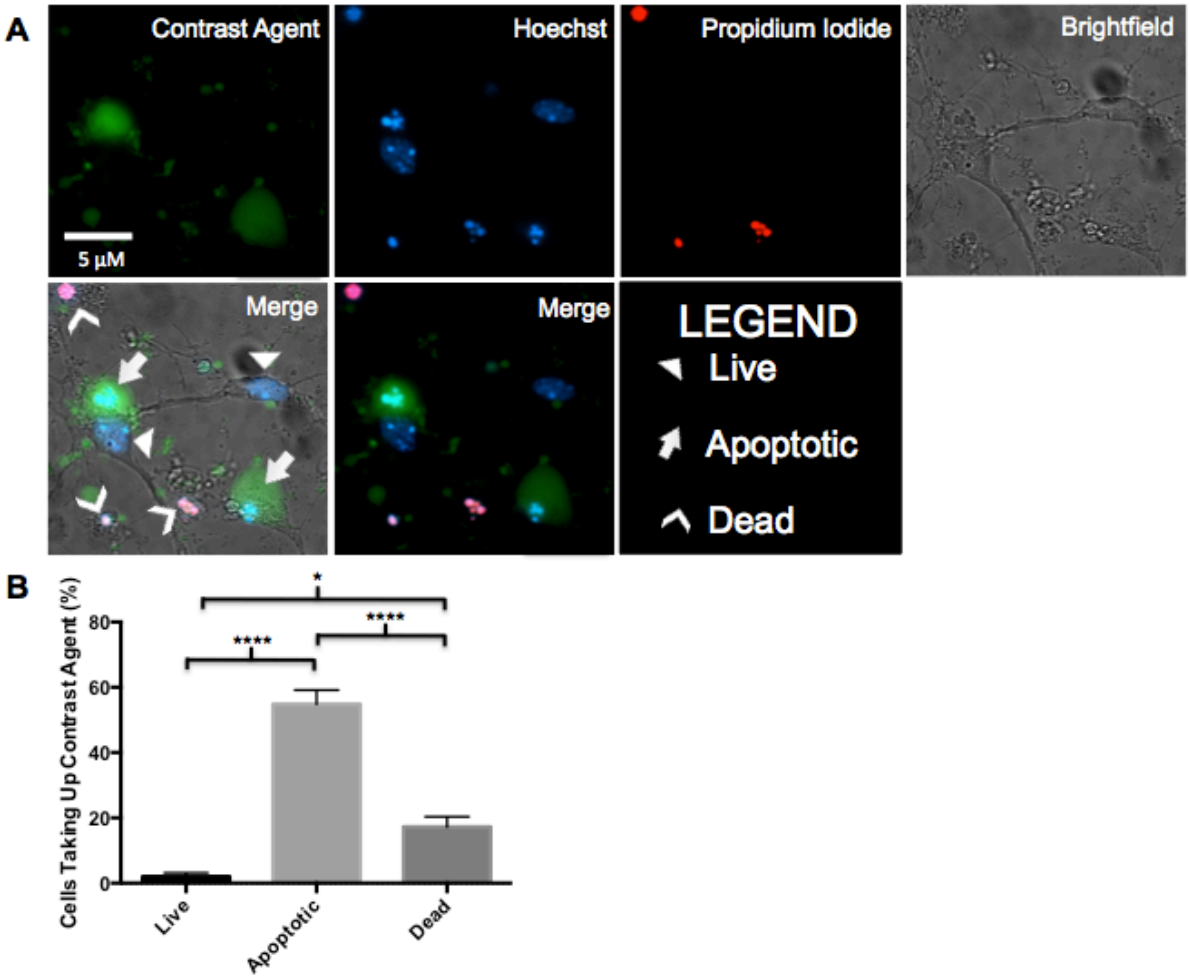

Figure 9. Apoptotic neurons selectively retain the contrast agent. Mouse primary cortical neurons were treated with CPT and exposed to 10 µM contrast agent for 4 hours. Neurons were stained with Hoechst 33342 and propidium iodide (PI) and imaged live using fluorescence microscopy. Cells exhibiting pyknotic and/or fragmented nuclei with negative PI staining were characterized as apoptotic. Cells displaying healthy diffuse nuclei with negative PI staining were characterized as healthy. Cells with positive PI staining, regardless of nuclear morphology, were considered dead. A. Neurons displaying typical apoptotic morphology preferentially take up and retain the contrast agent in comparison to healthy and dead neurons. B. Quantification of contrast agent uptake in live, apoptotic and dead neurons. Cell counting was performed to analyze the percentage of neurons retaining the contrast agent for each cell population. At least 200 cells were counted per experiment (n = 4). Error bars represent standard error of the mean. (* $p < 0.05$, **** $p < 0.0001$).

3.6 Apoptosis and Contrast Agent Uptake is Caspase-3 Dependent

Next we set out to confirm that uptake of our agent was due to caspase-3 activation. Cellular uptake and retention of the contrast agent was compared between neurons that were induced to undergo apoptosis and control neurons that were left untreated. To determine whether retention of the agent was truly dependent on cleavage by caspase-3, we also compared the uptake and retention of the contrast agent in neurons that were induced to undergo apoptosis in the presence of an irreversible caspase-3 inhibitor.

Primary neurons were treated with 10 μM CPT for 24 hours to induce apoptosis. To inhibit caspase-3 activation, 50 μM of the irreversible caspase-3 inhibitor Z-DEVD-FM was added 1 hour prior to the addition of CPT. Control neurons remained in regular culture medium 24 hours. During the last 4 hours of treatment, 10 μM of contrast agent was added to the neuron medium. At the end of the incubation period the neurons were washed and stained with Hoechst 33342 and PI. Cells were imaged live using fluorescence microscopy.

To compare agent uptake and retention between the three conditions the proportion of cells that retained the contrast agent was determined by counting the number of cells that appeared bright green and dividing by the total number of nuclei (Fig. 10B). At least 3000 cells from 3 independent experiments were counted in each condition to evaluate contrast agent uptake and retention. To correlate contrast agent retention and apoptosis, the proportion of apoptotic cells in each condition was determined. A minimum of 900 cells from 3 independent experiments were counted for each condition and the proportion of cells that were PI negative and displayed apoptotic nuclear morphology was scored (Fig. 10C).

In these experiments, 19 ± 3 % of the CPT-treated neurons retained the contrast agent in comparison to 2 ± 1 % of the untreated (control) neurons. Of the neurons treated with

CPT in the presence of a caspase-3 inhibitor, 3 ± 1 % of neurons retained the contrast agent. Statistical analysis revealed that significantly more cells retained the contrast agent when treated with the pro-apoptotic drug CPT compared to control neurons and neurons treated with CPT in the presence of a caspase-3 inhibitor ($p < 0.01$). To correlate agent retention to apoptosis, the proportion of apoptotic cells in each condition was quantified. CPT-treated, control, and CPT/caspase-3 inhibitor-treated neurons displayed 56 ± 5, 5 ± 1, and 10 ± 5 % apoptotic neurons, respectively. Statistical analysis revealed that significantly more CPT-treated neurons underwent apoptosis compared to control neurons and neurons treated with CPT in the presence of a caspase-3 inhibitor ($p < 0.0001$). These results demonstrate the ability of our contrast agent to detect apoptosis and indicate that uptake was dependent on caspase-3 activation.

To confirm that our agent was responding to apoptosis, we tested a variety of different stimuli that can induce apoptosis. We repeated the above experiment using MPP^+ to demonstrate the ability of our contrast agent to detect apoptosis in response to a different apoptotic stimulus. In contrast to the DNA damage-inducing agent CPT, MPP^+ inhibits complex I of the electron transport chain interfering with oxidative phosphorylation (Watanabe et al., 2005).

The experiment proceeded in the same manner as outlined above except to induce apoptosis neurons were exposed to 10 μM MPP^+ for 24 hours instead of CPT. At least 2400 cells from 3 independent experiments were counted in each condition to evaluate contrast agent uptake and retention. To evaluate apoptosis, at least 700 cells from 3 independent experiments were counted in each condition. Figure 11A shows representative images comparing the retention of the contrast agent in control, MPP^+-treated and MPP^+/caspase-3 inhibitor-treated neurons. Similar to the experiment conducted with CPT, a significantly larger proportion of neurons treated with MPP^+ retained the contrast agent compared to control or MPP^+/caspase-3 inhibitor-treated neurons (Fig. 11B; $p < 0.001$). In these experiments, 10 ± 1 % of MPP^+-treated neurons retained the contrast agent. This was in comparison to 2 ± 1 % of control neurons that

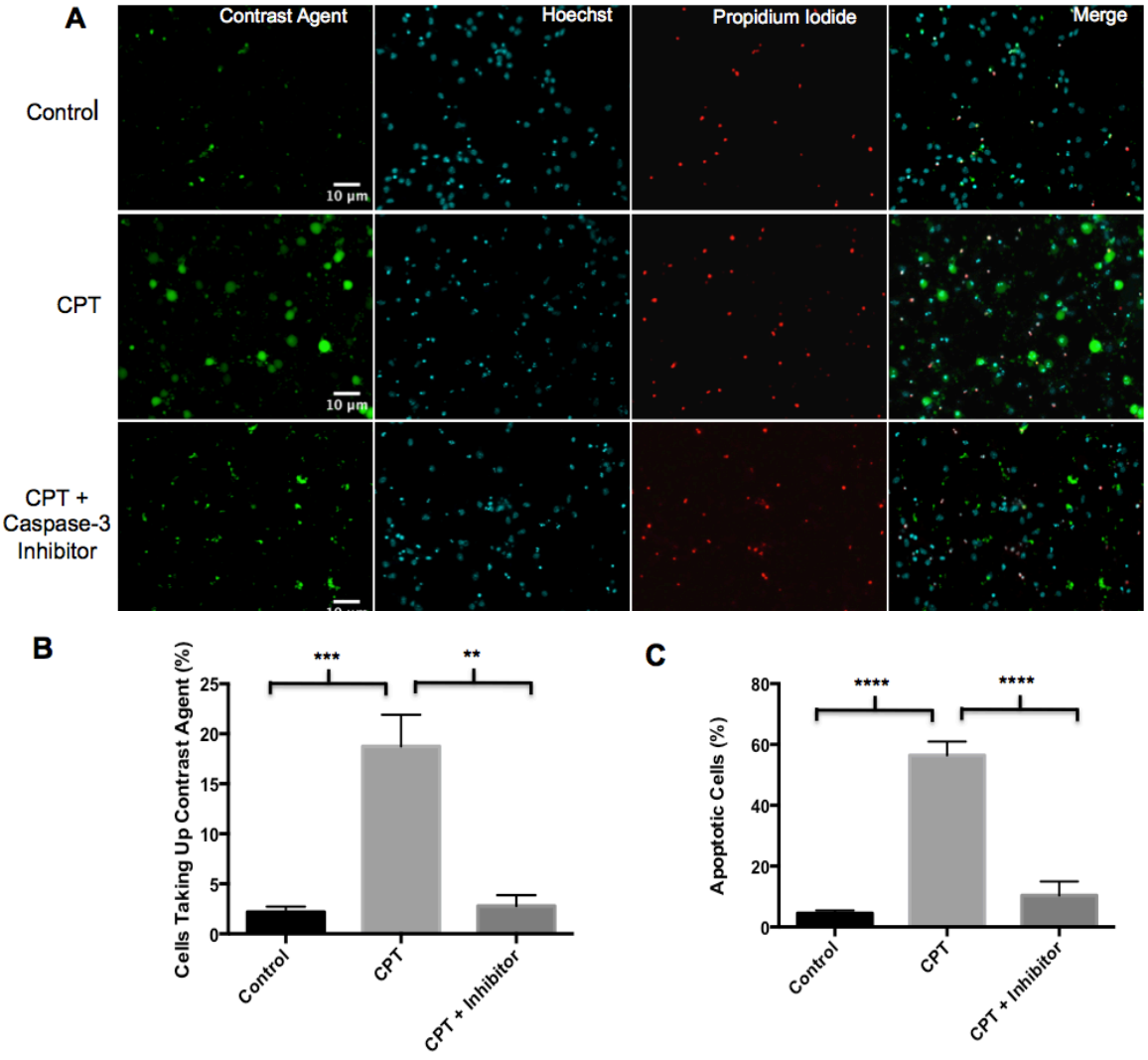

Figure 10. CPT increases the proportion of neurons retaining the contrast agent and is blocked with the addition of a caspase-3 inhibitor. Mouse primary cortical neurons were treated with either 10 µM CPT or 10 µM CPT plus 50 µM of the irreversible caspase-3 inhibitor Z-DEVD-FMK for 24 hours. During the last 4 hours of the incubation period cells were exposed to 10 µM contrast agent. Control neurons remained in regular culture medium. Neurons were stained with Hoechst 33342 and propidium iodide and imaged live using fluorescence microscopy. A. CPT-induced apoptosis increases the number of neurons retaining contrast agent. This effect is reversed in the presence of a caspase-3 inhibitor. B. Quantification of contrast agent uptake in control, CPT-treated, and CPT/inhibitor-treated neurons. Cell counting was performed to analyze the percentage of neurons taking up the contrast agent in the three groups. Images were acquired using a 20× lens and a minimum of 800 cells were counted per treatment per experiment (n = 3). C. Quantification of apoptotic neurons in control, CPT-treated, and

CPT/inhibitor-treated neurons. Cell counting was performed to determine the percentage of neurons that were PI negative and dispayed either condensed or fragmented nuclei. Images were acquired using a 40× lens and a minimum of 160 cells were analyzed per treatment per experiment (n = 3). Error bars represent standard error of the mean. (** $p < 0.01$, *** $p < 0.001$, **** $p < 0.0001$).

retained the contrast agent and 3 ± 1 % of neurons treated with MPP^+ in the presence of a caspase-3 inhibitor.

Again, the proportion of apoptotic cells in each condition paralleled contrast agent retention. As depicted in Figure 11C, there was a significantly greater proportion of apoptotic neurons when treated with MPP^+ compared to untreated control neurons or neurons treated with MPP^+ in the presence of a caspase-3 inhibitor ($p < 0.05$). When treated with MPP^+, 20 ± 3 % of neurons were apoptotic. This was in comparison to 5 ± 1 % of control neurons and 8 ± 2 % of neurons treated with MPP^+ in the presence of a caspase-3 inhibitor. These results further demonstrate the ability of our contrast agent to detect apoptosis.

3.7 Evaluation of Contrast Agent Retention in Necrotic Neurons

Radiolabeled Annexin V, the most successful method available at the current time for imaging apoptosis *in vivo* labels both apoptotic and necrotic cells and is unable to distinguish the two (Brauer, 2003; Blankenberg, 2008). Retention of our contrast agent relies on cleavage by caspase-3, and therefore should specifically label the apoptotic mode of cell death. To test this, we used N-methyl-D-aspartate (NMDA) to induce excitotoxicity in primary neurons and evaluated the retention of our contrast agent. Over-activation of NMDA receptors is toxic to neurons eventually leading to the disruption of ionic gradients across the plasma membrane. This causes cell swelling and eventually cell lysis (Wang and Qin, 2010).

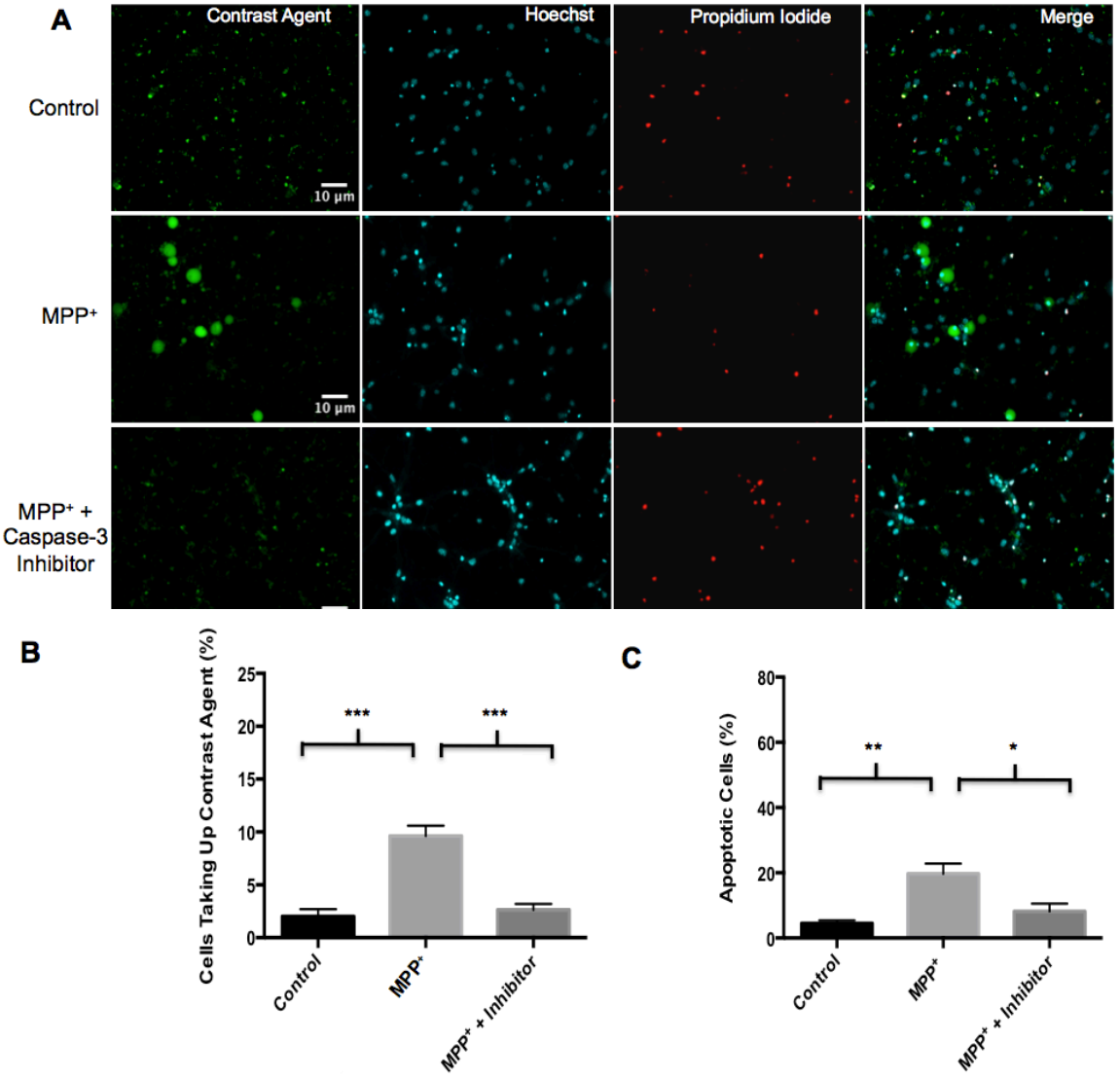

Figure 11. MPP^+ increases the proportion of neurons retaining the contrast agent and is blocked with the addition of a caspase-3 inhibitor. Mouse primary cortical neurons were treated with either 10 µM MPP^+ or 10 µM MPP^+ plus 50 µM of the irreversible caspase-3 inhibitor Z-DEVD-FMK for 24 hours. During the last 4 hours of the incubation period cells were exposed to 10 µM contrast agent. Control neurons remained in regular culture medium. Neurons were stained with Hoechst 33342 and propidium iodide and imaged live using fluorescence microscopy. A. MPP^+-induced apoptosis increases the number of neurons retaining contrast agent. This effect is reversed in the presence of a caspase-3 inhibitor. B. Quantification of contrast agent uptake in control, MPP^+-treated, and MPP^+/inhibitor-treated neurons. Cell counting was performed to analyze the percentage of neurons taking up the contrast agent in the three groups.

Images were acquired using a 20× lens and a minimum of 500 cells were counted per treatment per experiment (n = 3). C. Quantification of apoptotic neurons in control, MPP^+-treated, and MPP^+/inhibitor- treated neurons. Cell counting was performed to analyze the percentage of neurons showing either condensed or fragmented nuclei. Images were acquired using a 40× lens and a minimum of 170 cells were analyzed per treatment per experiment (n = 3). Error bars represent standard error of the mean. (* $p < 0.05$, ** $p < 0.01$, *** $p < 0.001$).

Primary cortical neurons were treated with 500 μM of NMDA for 6 hours to induce excitotoxicity. Control neurons remained in regular culture medium. During the last 4 hours of the treatment period 10 μM of the contrast agent was added. At the end of the incubation period the neurons were washed and stained with Hoechst 33342 and PI. Cells were imaged live using fluorescence microscopy (Fig. 12A and 12B). To compare agent uptake and retention between NMDA-treated and control neurons, the proportion of cells that retained the contrast agent was determined by counting the number of cells that appeared bright green and dividing by the total number of nuclei (Fig. 12C). At least 5000 cells from 4 independent experiments were counted in each condition to evaluate contrast agent uptake and retention. To quantify the number of necrotic cells in each condition, the proportion of PI positive cells was scored (Fig. 12D). At least 1500 cells from 4 independent experiments were counted in each condition to quantify necrosis.

Figure 12A displays representative images comparing contrast agent uptake and PI staining between NMDA-treated and control neurons. Figure 12B displays a representative image of neurons that have been treated with NMDA. The neurons imaged display cell swelling typical of excitotoxicity. The swollen cells do not retain the contrast agent. When treated with NMDA to induce excitotoxicity, 2 ± 1 % of neurons retained the contrast agent. This was no different from the 2 ± 1 % of untreated control neurons that retained the contrast agent. In comparison, 53 ± 4 % of NMDA treated neurons were PI positive compared to 30 ± 1 % of control neurons. The proportion of NMDA-treated PI positive cells was significantly

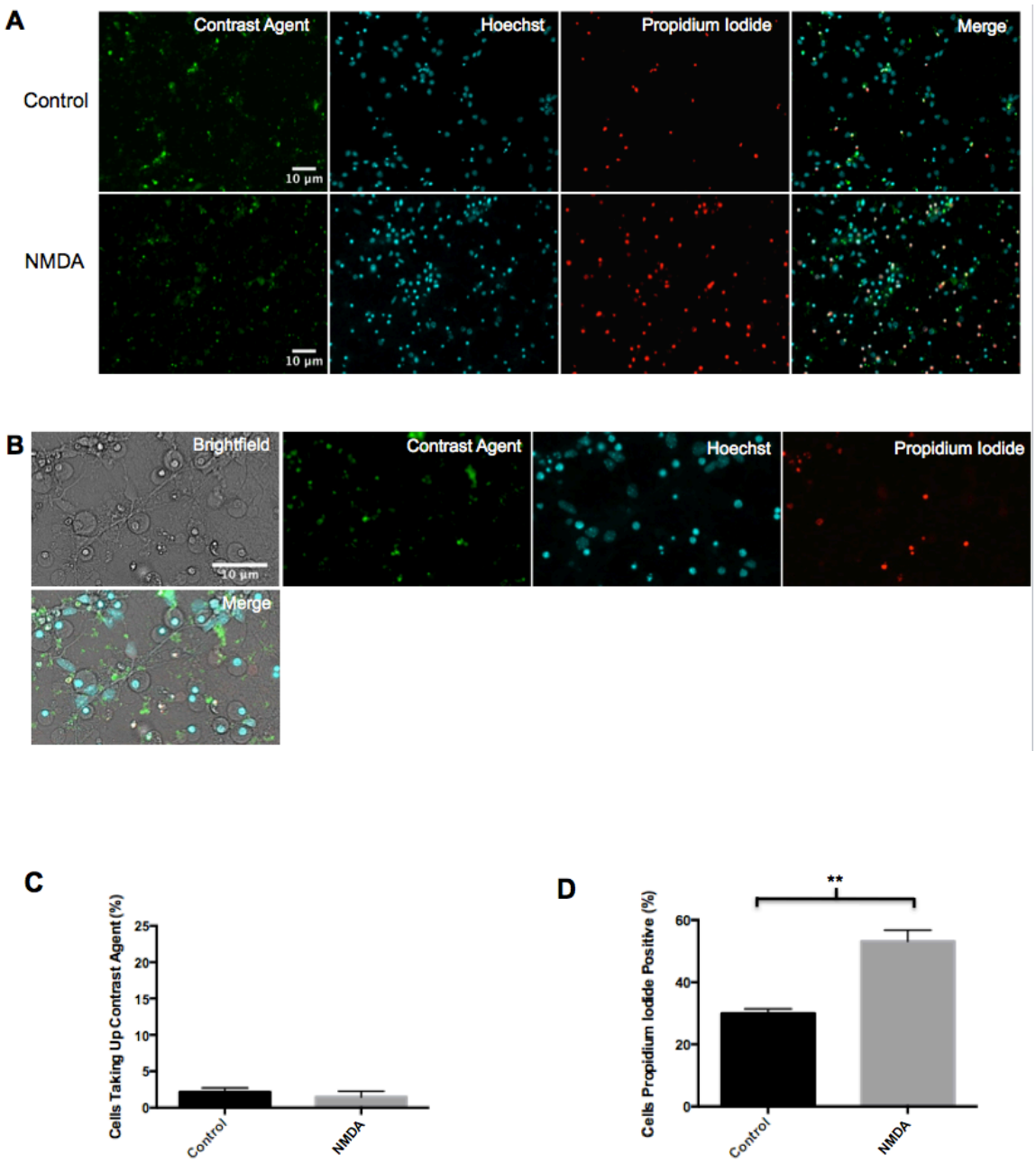

Figure 12. Necrotic cells do not retain the contrast agent. Mouse primary cortical neurons were treated with 500 µM of NMDA for 6 hours. For the last 4 hours 10 µM of contrast agent was added. Neurons were stained with Hoechst 33342 and propidium iodide (PI) and imaged live using fluorescence microscopy. A. Neurons treated with NMDA to induce excitotoxic cell death do not retain the contrast agent. B. Neurons treated with NMDA display cell swelling typical of excitotoxic cell death. C.

Quantification of contrast agent uptake in control and NMDA-treated neurons. Cell counting was performed to analyze the percentage of neurons taking up the contrast agent in the two groups. Images were acquired using a 20× lens and a minimum of 650 cells were counted per treatment per experiment (n = 4). D. Quantification of PI positive cells (dead) in control and NMDA-treated neurons. Images were acquired using a 40× lens and a minimum of 300 cells were analyzed per treatment per experiment (n = 4). Error bars represent standard error of the mean. (** $p < 0.01$).

greater than control neurons ($p < 0.01$). As there was no difference between contrast agent retention in excitotoxic cells and control cells, this indicates that our contrast agent does not label necrotic cells and provides additional support for its specificity for the detection of apoptosis.

3.8 1-Methyl-4-Phenyl-1,2,3,6-Tetrahydropyridine Mouse Model

To evaluate the ability of the contrast agent to detect apoptosis *in vivo*, the 1-methyl-4-phenyl-1,2,3,6-tetrahydropyridine (MPTP) mouse model of Parkinson's disease was used. MPTP is a potent neurotoxin that induces apoptosis in the dopaminergic neurons of the substantia nigra (Watanabe et al., 2005). For preliminary assessment of the contrast agent *in vivo*, agent uptake and retention were compared between MPTP-treated and control mice. Based on a protocol developed by Tatton and Kish, mice were given intraperitoneal injections of MPTP for five consecutive days. Control mice received saline injections. Three days after the final injection, mice were intravenously injected with 80 μL of 1 mM contrast agent. One mouse from each the MPTP-treated and control group were sacrificed at 1 and 2 hours to evaluate contrast agent distribution throughout the brain and analyze cell death.

Coronal sections were stained for tyrosine hydroxylase, a marker for dopaminergic neurons, to evaluate neuron loss in the substantia nigra (Fig. 13A). Dopaminergic cells were quantified by counting the number of tyrosine hydroxylase positive cells in the substantia nigra (Fig. 13B). The mean tyrosine hydroxylase positive cell count for control

brains was 49 ± 5 cells per section, compared to 27 ± 3 cells per section in the MPTP-treated brains. Statistical analysis revealed that there was a significant loss of tyrosine hydroxylase positive (dopaminergic) cells in MPTP-treated mice ($p < 0.001$).

Terminal deoxynucleotidyl transferase dUTP nick end labeling (TUNEL) staining was used to identify apoptotic cells in the substantia nigra (Fig. 13 C). Fluorescence microscopy was used to capture images across the substantia nigra of MPTP-treated and control mice and the number of TUNEL positive cells in the substantia nigra of each slice was quantified (Fig. 13 D). To our surprise, there were extremely few TUNEL positive cells within the substantia nigra of MPTP-treated brains 3 days after the last MPTP injection. The mean TUNEL positive cell count for MPTP-treated brains was 1.5 ± 0.25 cells per section, compared to 0.75 ± 0.3 cells per section in control brains. The number of TUNEL positive cells in MPTP-treated and control mice were not statistically different. Additionally, examination of nuclear morphology revealed healthy looking nuclei in both MPTP-treated and control mice.

Finally, contrast agent distribution was analyzed by imaging brain sections using fluorescence microscopy. Contrast agent distribution was compared between MPTP-treated and control mice sacrificed at 1 and 2 hours. Additionally, one MPTP-treated and one control mouse were not injected with contrast agent to compare background fluorescence. To compare agent uptake, images were acquired using the green channel of a fluorescence microscope (Fig. 13E). We attempted to measure fluorescence, however, there was substantial background florescence even in the control, non-injected mouse, and therefore we were unable to produce convincing images of a difference in signal between the injected and control animals.

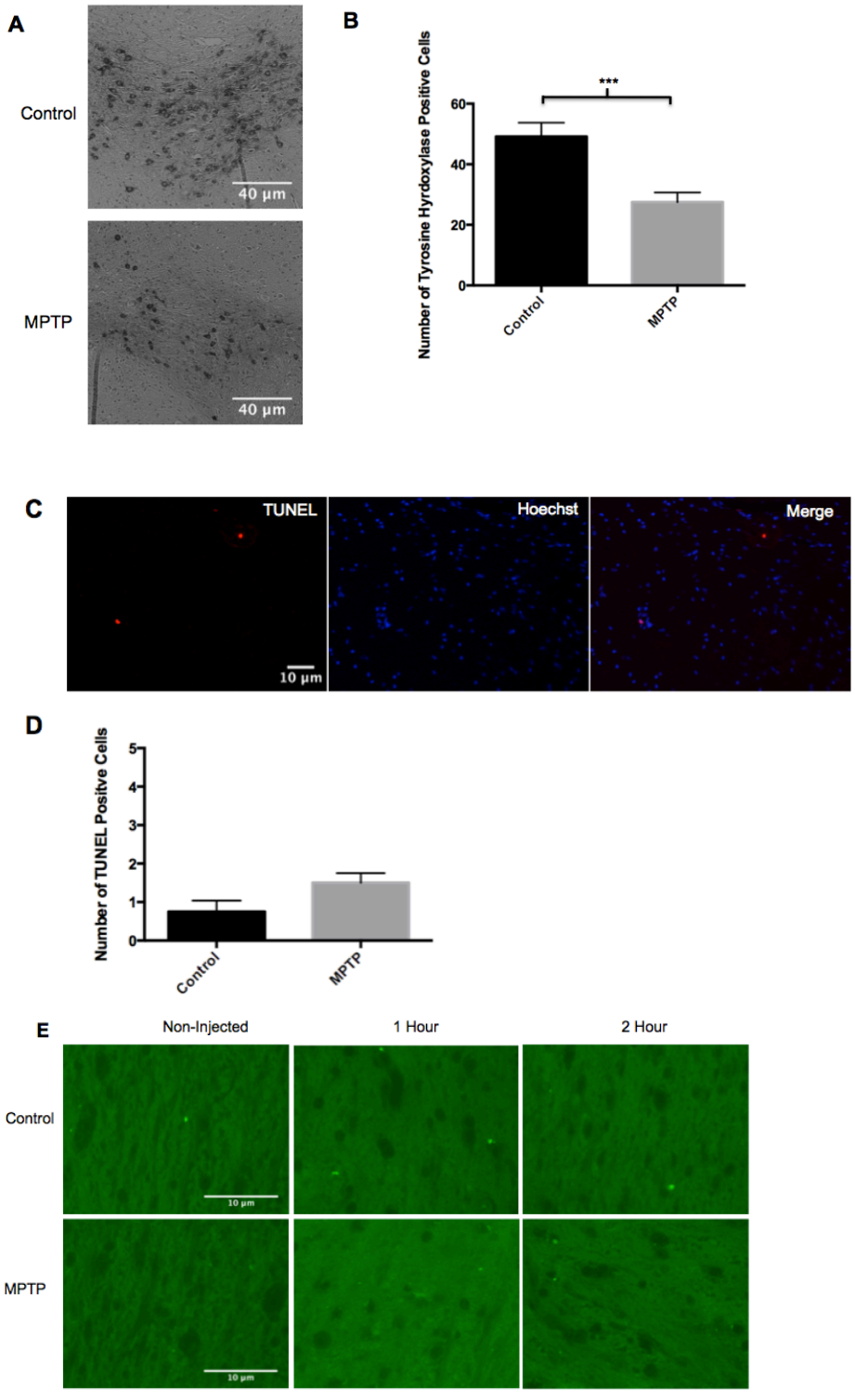

Figure 13. Evaluation of contrast agent uptake in MPTP-treated and control mice. Mice were injected IP with MPTP for 5 consecutive days to induce apoptosis in the

dopaminergic neurons of the substantia nigra. Control mice received saline injections. Three days after the last injection mice received an IV injection of 80 μM of 1 mM contrast agent. Mice were sacrificed at 1 and 2 hours post-injection to analyze contrast agent distribution and cell death throughout the brain. One mouse from each group was not injected with contrast agent to compare background fluorescence. Coronal sections were stained with tyrosine hydroxylase to identify dopaminergic neurons in the substantia nigra. Apoptosis was evaluated by TUNEL staining. Contrast agent distribution was analyzed by imaging the substantia nigra using fluorescence microscopy. A. Representative images displaying tyrosine hydroxylase staining in half of the substantia nigra in MPTP-treated and control mice. B. Dopaminergic cells were quantified by counting the number of tyrosine hydroxylase positive cells in the substantia nigra. Three mice were analyzed from each condition and at least four sections were analyzed per mouse (n=3). C. Representative image displaying two TUNEL positive cells in the substantia nigra of an MPTP-treated mouse. D. Apoptosis was evaluated by counting the number of TUNEL positive cells in the substantia nigra. Three mice were analyzed from each condition and at least four sections were analyzed per mouse (n=3). E. Representative images acquired in the green channel to visualize the contrast agent (n=1). Error bars represent standard error of the mean. (** $p < 0.001$).

Chapter 4

4 Discussion

We have developed a novel contrast agent for the *in vivo* detection of apoptosis. The primary goal of this study was to test the ability of our contrast agent to label apoptotic cells in culture and we hoped to also explore its potential to detect apoptosis *in vivo*. By inducing apoptosis in mouse primary cortical neurons, we demonstrated the ability to label apoptotic cells in culture. When we analyzed neurons on a cell-by-cell basis, our contrast agent selectively labeled apoptotic cells, and was not retained within healthy or necrotic cells. Additionally, retention of the contrast agent was eliminated when apoptosis was blocked with a caspase-3 inhibitor. Finally, treatment of neurons with NMDA to induce excitotoxicity, demonstrated the ability of our agent to specifically label the apoptotic mode of cell death over the necrotic mode of cell death.

To test our contrast agent *in vivo*, the 1-methyl-4-phenyl-1,2,3,6-tetrahydropyridine (MPTP) mouse model of Parkinson's disease was used to induce apoptosis in the dopaminergic neurons of the substantia nigra (SN). MPTP-treated and control mice were injected intravenously with our contrast agent and sacrificed to evaluate contrast agent distribution and cell death. While we were able to induce a significant loss of dopaminergic neurons in MPTP-treated compared to control mice, at the time the mice were sacrificed, there was little evidence of apoptosis. Fluorescence microscopy was used to evaluate contrast agent distribution throughout the brains. Unfortunately, there was substantial background autofluorescence even in uninjected mice and we were not able to identify any cells with significant retention of the agent within the SN of MPTP-treated or control mice.

4.1 Apoptosis in Tumor Cell Lines

Initially we had invested significant effort in using immortalized neural cell lines to evaluate the ability of our contrast agent to label apoptotic cells in culture. This would have provided easy access to large numbers of cells for our studies. Unfortunately, it proved to be very difficult to induce apoptosis in our cell lines, even when using 5 times the published dose of several agents. Therefore, we had to switch to primary neuronal cultures. While this was technically more demanding and produced fewer cells, these cells underwent apoptosis and necrosis easily.

4.2 Cell Viability Studies

Incubation of primary cortical neurons with 10 μM contrast agent for up to 24 hours was found to have no affect on cell viability. While further studies will be needed to demonstrate the safety of our agent *in vivo*, this cellular work provides a promising indication of our agent's safety. In comparison, TcapQ, a caspase-activatable probe developed by Bullok *et al.* for the detection of apoptosis was found to significantly affect the viability of HeLa cells in culture. This agent produced a 50% loss of cell viability when incubated with 10 μM for 24 hours and a 90% loss of cell viability when incubated with 25 μM for 24 hours (Bullok et al., 2007). This demonstrates the high toxicity that some intracellular enzymatic probes may confer and highlights the negligible toxicity of our agent *in vitro*.

4.3 Apoptotic Neurons Selectively Retain the Contrast Agent

Individual cell analysis revealed that when our contrast agent was exposed to a combination of apoptotic, living and dead cells, it was selectively retained only within apoptotic cells. The importance of this result is twofold. First it indicates that our agent accumulates in cells undergoing apoptosis, producing detectable contrast. Second, it demonstrates the specificity of our agent to selectively label apoptotic cells and distinguish them from healthy and dead cells. These results are very important when

evaluating the potential of our contrast agent to detect apoptosis *in vivo*. The selective accumulation of our agent in apoptotic cells suggests its ability to detect apoptosis in pathological processes *in vivo* where there is an increase in apoptosis.

When we analyzed contrast agent uptake in individual neurons, approximately 50% of apoptotic neurons retained the contrast agent and appeared bright green. We anticipate that only half of the apoptotic cells were labeled due to the asynchronous fashion and rapid progression of apoptosis. In our study, cells characterized as apoptotic demonstrated chromatin condensation and/or nuclear fragmentation while maintaining membrane integrity. Video microscopy studies have revealed that the execution phase of apoptosis—where the morphological changes such as chromatin condensation and nuclear fragmentation are observed—proceeds very rapidly and occurs within a 2-hour time span (Messam and Pittman, 1998). Additionally, initiation of the execution phase is highly asynchronous and at any time point only a small fraction of cells are entering the execution phase of apoptosis (Messam and Pittman, 1998). The result is a relatively short time window at which you can "catch" and label an apoptotic cell.

The length of contrast agent exposure is also an important variable. In our study, unlabeled cells that display apoptotic morphology have likely just entered the execution phase of apoptosis and have not had enough time to accumulate contrast agent. In our optimization studies, we saw an increase in agent retention when neurons were exposed to the contrast agent for longer periods of time. This suggests that it takes a sufficient amount of time to accumulate enough agent in an apoptotic cell before it can be visualized by fluorescence microscopy.

The induction of secondary necrosis in very late apoptotic cells will also limit the proportion of apoptotic cells labeled by our contrast agent. *In vitro*, without the presence of macrophages, apoptosis ultimately concludes in a process known as secondary necrosis, where the cell lyses and releases its cellular contents (Silva, 2010). In these cells, any accumulated agent would leak out. *In vivo*, where macrophages exist to engulf the apoptotic cells, the signal would be retained within the bodies of macrophages.

4.4 Apoptosis and Contrast Agent Retention is Caspase-3 Dependent

We further evaluated the ability of our contrast agent to detect apoptosis by comparing uptake between three different populations: i) neurons induced to undergo apoptosis, ii) neurons induced to undergo apoptosis in the presence of a caspase-3 inhibitor, and iii) healthy control neurons. Evaluation of contrast agent uptake and retention demonstrated that a significantly greater proportion of neurons were labeled in conditions where they were induced to undergo apoptosis in comparison to control neurons. Additionally, when apoptosis was blocked with the addition of a caspase-3 inhibitor, we did not observe an increase in the number of cells labeled by our agent. This was demonstrated in two separate studies that each used a different apoptotic stimulus to induce apoptosis. These results indicate that our agent is capable of detecting when there is an increase in apoptosis *in vitro*. They also indicate that apoptosis, and subsequent retention of our contrast agent, is dependent on caspase-3 activation and provide additional support for the ability or our agent to label apoptotic cells.

When neurons were treated with 1-methyl-4-phenylpyridinium (MPP^+) there was a small increase the number of cells undergoing apoptosis (20% of MPP^+-treated neurons were apoptotic compared to 5% of control neurons). Despite the small increase in apoptotic cells, we still observed a significant increase in the number of neurons labeled by our agent. This ability to detect minor increases in apoptosis demonstrates the sensitivity of our agent. This is very important when it comes to detecting apoptosis *in vivo*, where in pathological situations there may only be a slight increase in the number of cells undergoing apoptosis. The natural rate of apoptosis in normal tissue is less than 2% (Brauer, 2003). In chronic diseases, where apoptosis is involved, the proportion of cells undergoing apoptosis at any one time is unlikely to exceed 10% (Brauer, 2003). Consequently, when developing a contrast agent for the detection of apoptosis, it is important that the agent is sensitive and capable of detecting very minor fluctuations or increases in apoptosis.

4.5 Necrotic Neurons Do Not Retain the Contrast Agent

When we treated primary cortical neurons with NMDA to induce excitotoxicity, a form of necrotic cell death, our contrast agent was not retained. This indicates that our contrast agent does not label necrotic cells and demonstrates the specificity of or agent for the apoptotic mode of cell death. At present, the most promising agent available for detecting apoptosis *in vivo* is radiolabelled Annexin V (Blankenberg, 2008; Tait, 2008; Niu and Chen, 2010). Annexin V has an extremely high affinity for phosphatidyl serine (PS), a phospholipid that is usually restricted to the inner leaflet of the plasma membrane but becomes exposed when cells undergo apoptosis (Martin et al., 1995). While this agent has made it to multiple clinical trials in humans and demonstrates some ability to detect apoptosis in vivo, it has a major limitation (Blankenberg et al., 1999; Belhocine et al., 2002). In addition to binding externalized PS on apoptotic cells, Annexin V also binds to PS on necrotic cells that have lost their membrane integrity (van Engeland et al., 1998). As a result, this agent is unable to discriminate between apoptosis and necrosis. While marketed as an agent for the detection of apoptosis, this probe really just detects cell death, both apoptotic and necrotic.

Our probe was designed to detect enzymatic caspase-3 activity. Activation of caspase-3 is unique to apoptotic cell death, and therefore provides a desirable target for the specific detection of apoptosis. Our results demonstrating that necrotic cells do not retain our contrast agent provide convincing evidence for the ability of our agent to specifically detect apoptosis. The ability to specifically detect apoptosis *in vivo* would provide a very valuable research tool for studying apoptosis. A probe allowing us to specifically image apoptosis in living organisms would help us further our understanding of how apoptosis contributes to a variety of pathological processes.

4.6 1-Methyl-4-Phenyl-1,2,3,6-Tetrahydropyridine Mouse Model

For the preliminary assessment of our contrast agent *in vivo*, mice were injected with MPTP to induce apoptosis in the dopaminergic neurons of the SN. Originally, we hoped

that this would be an ideal system, because it produced neuronal loss almost exclusively by apoptosis (Tatton and Kish, 1997). MPTP-treated and control mice were then injected intravenously with 80 μL of 1 mM contrast agent. Finally, mice were sacrificed at 1 and 2 hours post injection and histological sections of the SN were generated to analyze contrast agent distribution and cell death.

Tyrosine hydroxylase was used to stain and visualize the dopaminergic neurons of the SN. Cell counts analyzing the number of tyrosine hydroxylase positive cells revealed that we were successfully able to induce neuron death in the SN of MPTP-treated mice. Terminal deoxynucleotidyl transferase dUTP nick end labeling (TUNEL) was then used to identify apoptotic cells with DNA fragmentation. When we analyzed brain sections of MPTP-treated mice, only 1-2 cells in each section of the SN were TUNEL positive. Due to the extreme toxicity of MPTP, we were required by our Health and Safety Officer to wait 3 days after the last MPTP injection for the toxic compound to clear from the mice before we were able to inject them with our contrast agent. Accordingly, this may be one of the reasons we did not observe significant apoptosis. At the time at which we injected the mice with our contrast agent and then subsequently sacrificed them, it was likely too late to detect any neurons undergoing apoptosis. In retrospect, we realized that it has been demonstrated that apoptosis peaks 24 hours after the final MPTP injection (Tatton and Kish, 1997). However, when we examined this data in detail, even 24 hours after the last MPTP injection, when apoptosis is documented to peak, the number of neurons undergoing apoptosis is extremely low (Tatton and Kish, 1997). Therefore, it appears that this system is not robust enough (does not produce enough synchronized apoptosis) to be useful for *in vivo* studies.

To evaluate the distribution of the contrast agent throughout the brain, we used the green channel of a fluorescence microscope. Looking at the SN, we were not able to identify any cells that retained our contrast agent in MPTP-treated or control mice. There are a number of possibilities for why we were unable to detect our contrast agent. One possibility is that the contrast agent was not able to cross the blood brain barrier (BBB)

and never gained access to the SN. However, previous work from our lab using a contrast agent with the exact same structure but different enzymatic cleavage site was detected in the brains of mice within 60 minutes of injection (Ta et al., 2013). It is therefore unlikely that the current contrast agent was not able to penetrate the BBB and make it into the central nervous system vasculature.

Another possible explanation for the lack of detectable contrast agent is that it was washed away during perfusion or subsequent preparation of the brain tissue sections. Our contrast agent is extremely small and does not fix well. When we attempted to fix neurons that had retained our contrast agent *in vitro*, it is possible that the contrast agent did not fix well and was washed away. Therefore, we think it is highly likely that some of the agent was lost during perfusion and tissue preparation. In the future, it may be wise to snap freeze unperfused brains and then analyze agent distribution.

It is also possible that our contrast is present throughout the substantia nigra, but we are simply unable to detect it using fluorescence microscopy. The background fluorescence in the green channel was high, even in uninjected mice. It is possible, therefore, that we are unable to detect fluorescence coming from our contrast agent over the background. This could be overcome by changing the colour of the fluorophore in our contrast agent or by switching to a more sensitive imaging modality. Another way of boosting the signal intensity would be to deliver consecutive injections of our contrast agent to mice or by administering the agent via intraperitoneal injections, thereby allowing more time for the agent to accumulate in apoptotic cells.

4.7 Future Studies

In the future, it will be necessary to switch to a different model of apoptosis, where there are a larger proportion of cells undergoing apoptosis at any one time. Although cerebral stroke models induce a mixture of apoptosis and necrosis, they may provide a better model for testing our contrast agent *in vivo*. Histological analyses from cerebral stroke models in rats have revealed widespread apoptosis and TUNEL staining (Linnik et al.,

1995; Chen et al., 1997). Chen *et* al. demonstrated that 72 hours after a transient 1-hour middle cerebral artery occlusion, hundreds of cells within the piriform cortex, caudate nucleus and putamen are TUNEL positive within the rat brain. This suggests that a cerebral stroke model may provide a more robust model (greater number of cells undergoing apoptosis at the same time) for inducing apoptosis *in vivo*.

Following the establishment of an adequate model for apoptosis *in vivo*, it will be necessary to establish the appropriate timing and dose for the injection of our contrast agent. As mentioned earlier, we may find it beneficial to administer multiple doses of our contrast agent, allowing for greater accumulation in apoptotic cells. Additionally, as apoptosis is rare a rare event *in vivo,* even under pathological circumstances, we may find ourselves moving towards a more sensitive imaging modality, such as positron emission tomography (PET) (Brauer, 2003).

4.8 Conclusion

This thesis presents the first step in the development of a contrast agent to detect apoptosis *in vivo*. We demonstrated the ability to reliably label apoptotic cells generated using several different methods. In addition, we demonstrated the selectivity or our agent for apoptotic cells over necrotic or lysed cells. Unfortunately, we were unable to evaluate the ability of our contrast agent to detect apoptosis *in vivo* using MPTP to induce apoptosis in the dopaminergic neurons of the SN in mice. In the future, it will be necessary to switch to a new model of apoptosis with more robust cell death. Nonetheless, we have provided convincing data for the ability to label apoptotic cells *in vitro* using our contrast agent and believe it holds the potential to provide a non-invasive method to image apoptosis *in vivo*. We hope that this imaging technique will be very useful in the assessment and early diagnosis of neurodegenerative disease.

References

Agarwal ML, Taylor WR, Chernov M V., Chernova OB, Stark GR (1998) The p53 network. J Biol Chem 273:1–4.

Alauddin MM (2012) Positron emission tomography (PET) imaging with (18)F-based radiotracers. Am J Nucl Med Mol Imaging 2:55–76 Available at: http://www.pubmedcentral.nih.gov/articlerender.fcgi?artid=3478111&tool=pmcentrez&rendertype=abstract.

Alnemri ES, Litwack G (1990) Activation of internucleosomal DNA cleavage in human CEM lymphocytes by glucocorticoid and novobiocin: Evidence for a non-Ca2+-requiring mechanism(s). J Biol Chem 265:17323–17333.

Ashkenazi A (2002) Targeting death and decoy receptors of the tumour-necrosis factor superfamily. Nat Rev Cancer 2:420–430.

Balasubramanian K, Schroit AJ (2003) Aminophospholipid asymmetry: A matter of life and death. Annu Rev Physiol 65:701–734.

Balcer-Kubiczek EK (2012) Apoptosis in radiation therapy: A double-edged sword. Exp Oncol 34:277–285.

Basu S, Kwee TC, Surti S, Akin E a., Yoo D, Alavi A (2011) Fundamentals of PET and PET/CT imaging. Ann N Y Acad Sci 1228:1–18.

Belhocine T, Steinmetz N, Hustinx R, Bartsch P, Jerusalem G, Seidel L, Rigo P, Green A (2002) Increased uptake of the apoptosis-imaging agent 99mTc recombinant human annexin V in human tumors after one course of chemotherapy as a predictor of tumor response and patient prognosis. Clin Cancer Res 8:2766–2774.

Blankenberg FG (2008) In vivo detection of apoptosis. J Nucl Med 49 Suppl 2:81S – 95S.

Blankenberg FG, Kalinyak J, Liu L, Koike M, Cheng D, Goris ML, Green A, Vanderheyden JL, Tong DC, Yenari MA (2006) 99mTc-HYNIC-annexin V SPECT imaging of acute stroke and its response to neuroprotective therapy with anti-Fas ligand antibody. Eur J Nucl Med Mol Imaging 33:566–574.

Blankenberg FG, Katsikis PD, Tait JF, Davis RE, Naumovski L, Ohtsuki K, Kopiwoda S, Abrams MJ, Darkes M, Robbins RC, Maecker HT, Strauss HW (1998) In vivo detection and imaging of phosphatidylserine expression during programmed cell death. Proc Natl Acad Sci U S A 95:6349–6354.

Blankenberg FG, Katsikis PD, Tait JF, Davis RE, Naumovski L, Ohtsuki K, Kopiwoda S, Abrams MJ, Strauss HW (1999) Imaging of apoptosis (programmed cell death) with 99mTc annexin V. J Nucl Med 40:184–191.

Bort G, Catoen S, Borderies H, Kebsi A, Ballet S, Louin G, Port M, Ferroud C (2014) Gadolinium-based contrast agents targeted to amyloid aggregates for the early diagnosis of Alzheimer's disease by MRI. Eur J Med Chem 87:843–861 Available at: http://linkinghub.elsevier.com/retrieve/pii/S0223523414009428.

Bortner CD, Cidlowski J a. (1998) A necessary role for cell shrinkage in apoptosis. Biochem Pharmacol 56:1549–1559.

Bossy-Wetzel E, Green DR (2000) Assays for cytochrome c release from mitochondria during apoptosis. ACADEMIC PRESS. Available at: http://dx.doi.org/10.1016/S0076-6879(00)22024-7.

Brauer M (2003) In vivo monitoring of apoptosis. Prog Neuro-Psychopharmacology Biol Psychiatry 27:323–331.

Bressenot A, Marchal S, Bezdetnaya L, Garrier J, Guillemin F, Plénat F (2009) Assessment of apoptosis by immunohistochemistry to active caspase-3, active caspase-7, or cleaved PARP in monolayer cells and spheroid and subcutaneous xenografts of human carcinoma. J Histochem Cytochem 57:289–300.

Brill a, Torchinsky a, Carp H, Toder V (1999) The role of apoptosis in normal and abnormal embryonic development. J Assist Reprod Genet 16:512–519.

Broughton BRS, Reutens DC, Sobey CG (2009) Apoptotic mechanisms after cerebral ischemia. Stroke 40.

Bullmore E, Bullmore E, Sporns O, Sporns O (2009) Complex brain networks: graph theoretical analysis of structural and functional systems. Nat Rev Neurosci 10:186–198 Available at: citeulike-article-id\n4025955\nhttp\n//dx.doi.org/10.1038/nrn2575.

Bullok KE, Maxwell D, Kesarwala AH, Gammon S, Prior JL, Snow M, Stanley S, Piwnica-Worms D (2007) Biochemical and in vivo characterization of a small, membrane-permeant, caspase-activatable far-red fluorescent peptide for imaging apoptosis. Biochemistry 46:4055–4065.

Cai SX, Zhang HZ, Guastella J, Drewe J, Yang W, Weber E (2001) Design and synthesis of rhodamine 110 derivative and caspase-3 substrate for enzyme and cell-based fluorescent assay. Bioorganic Med Chem Lett 11:39–42.

Caravan P, Ellison JJ, McMurry TJ, Lauffer RB (1999) Gadolinium(III) Chelates as MRI Contrast Agents: Structure, Dynamics, and Applications. Chem Rev 99:2293–2352 Available at: http://www.ncbi.nlm.nih.gov/pubmed/11749483.

Charles I, Khalyfa A, Kumar DM, Krishnamoorthy RR, Roque RS, Cooper N, Agarwal N (2005) Serum deprivation induces apoptotic cell death of transformed rat retinal ganglion cells via mitochondrial signaling pathways. Investig Ophthalmol Vis Sci 46:1330–1338.

Chen J, Jin K, Chen M, Pei W, Kawaguchi K, Greenberg D a, Simon RP (1997) Early detection of DNA strand breaks in the brain after transient focal ischemia: implications for the role of DNA damage in apoptosis and neuronal cell death. J Neurochem 69:232–245.

Choi DW (1996) Ischemia-induced neuronal apoptosis. Curr Opin Neurobiol 6:667–672.

Chong A (2010) Common hand conditions. Singapore Med J 2011:965–971 Available at: http://www.bssh.ac.uk/patients/commonhandconditions.

Clutton S (1997) The importance of oxidative stress in apoptosis. Br Med Bull 53:662–668.

Cohen GM (1997) Caspases: the executioners of apoptosis. Biochem J 326 (Pt 1:1–16.

Collins J a, Schandi C a, Young KK, Vesely J, Willingham MC (1997) Major DNA fragmentation is a late event in apoptosis. J Histochem Cytochem 45:923–934.

Daniel PT, Sturm I, Ritschel S, Friedrich K, Dörken B, Bendzko P, Hillebrand T (1999) Detection of genomic DNA fragmentation during apoptosis (DNA ladder) and the simultaneous isolation of RNA from low cell numbers. Anal Biochem 266:110–115.

Davie C a. (2008) A review of Parkinson's disease. Br Med Bull 86:109–127.

De Saint-Hubert M, Prinsen K, Mortelmans L, Verbruggen A, Mottaghy FM (2009) Molecular imaging of cell death. Methods 48:178–187 Available at: http://dx.doi.org/10.1016/j.ymeth.2009.03.022.

Didenko V V., Hornsby PJ (1996) Presence of double-strand breaks with single-base 3' overhangs in cells undergoing apoptosis but not necrosis. J Cell Biol 135:1369–1376.

Duke RC, Chervenak R, Cohen JJ (1983) Endogenous endonuclease-induced DNA fragmentation: an early event in cell-mediated cytolysis. Proc Natl Acad Sci U S A 80:6361–6365.

Ehrenberg B, Montana V, Wei MD, Wuskell JP, Loew LM (1988) Membrane potential can be determined in individual cells from the nernstian distribution of cationic dyes. Biophys J 53:785–794.

Elmore S (2007) Apoptosis: a review of programmed cell death. Toxicol Pathol 35:495–516.

Fadok VA, Voelker R, Campbell PA, Bratton DL, Henson PM, Cohen JJ (1992) EXPOSURE OF PHOSPHATIDYLSERINE ON THE SURFACE OF APOPTOTIC LYMPHOCYTES TRIGGERS SPECIFIC RECOGNITION AND REMOVAL BY MACROPHAGES '.

Galehdar Z, Swan P, Fuerth B, Callaghan SM, Park DS, Cregan SP (2010) Neuronal apoptosis induced by endoplasmic reticulum stress is regulated by ATF4-CHOP-mediated induction of the Bcl-2 homology 3-only member PUMA. J Neurosci 30:16938–16948.

Gambhir SS (2002) Molecular imaging of cancer with positron emission tomography. Nat Rev Cancer 2:683–693.

Gavrieli Y, Sherman Y, Scmuel A. Ben-Sasson (1992) Identification of Programmed Cell Death In Situ. Cell 119:493–501.

Gottlieb R a, Nordberg J, Skowronski E, Babior BM (1996) Apoptosis induced in Jurkat cells by several agents is preceded by intracellular acidification. Proc Natl Acad Sci U S A 93:654–658.

Green DR, Kroemer G (2004) The pathophysiology of mitochondrial cell death. Science 305:626–629.

Hagmann P, Cammoun L, Gigandet X, Meuli R, Honey CJ, Van Wedeen J, Sporns O (2008) Mapping the structural core of human cerebral cortex. PLoS Biol 6:1479–1493.

Harmon B V, Corder a M, Collins RJ, Gobé GC, Allen J, Allan DJ, Kerr JF (1990) Cell death induced in a murine mastocytoma by 42-47 degrees C heating in vitro:

evidence that the form of death changes from apoptosis to necrosis above a critical heat load. Int J Radiat Biol 58:845–858.

Heikkila RE, Hess A, Duvoisin RC (1984) Dopaminergic neurotoxicity of 1-methyl-4-phenyl-1,2,5,6-tetrahydropyridine in mice. Science (80-) 224:1451–1453.

Heiskanen KM, Bhat MB, Wang HW, Ma J, Nieminen AL (1999) Mitochondrial depolarization accompanies cytochrome c release during apoptosis in PC6 cells. J Biol Chem 274:5654–5658.

Hossain MA, Kim DH, Jang JY, Kang YJ, Yoon JH, Moon JO, Chung HY, Kim GY, Choi YH, Copple BL, Kim ND (2012) Aspirin enhances doxorubicin-induced apoptosis and reduces tumor growth in human hepatocellular carcinoma cells in vitro and in vivo. Int J Oncol 40:1636–1642.

Huerta S, Goulet EJ, Huerta-Yepez S, Livingston EH (2007) Screening and Detection of Apoptosis. J Surg Res 139:143–156.

Ito D, Walker JR, Thompson CS, Lin W, Veselits ML, Hakim AM, Fienberg A a, Thinakaran G, Moroz I (2004) Characterization of Stanniocalcin 2 , a Novel Target of the Mammalian Unfolded Protein Response with Cytoprotective Properties Characterization of Stanniocalcin 2 , a Novel Target of the Mammalian Unfolded Protein Response with Cytoprotective Properties. 24:9456–9469.

James ML, Gambhir SS (2012) A Molecular Imaging Primer: Modalities, Imaging Agents, and Applications. Physiol Rev 92:897–965.

Janicke RU (1998) Caspase-3 Is Required for DNA Fragmentation and Morphological Changes Associated with Apoptosis. J Biol Chem 273:9357–9360.

Jenner P, Olanow CW (1998) Understanding Cell Death in Parkinson ' s Disease. :72–84.

Johnson L V, Walsh ML, Bockus BJ, Chen LB (1981) Monitoring of Relative Mitochondrial-Membrane Potential in Living Cells By Fluorescence Microscopy. J Cell Biol 88:526–535 Available at: <Go to ISI>://A1981LE20200007.

Jolly PD, Smith PR, Heath D a, Hudson NL, Lun S, Still L a, Watts CH, McNatty KP (1997) Morphological evidence of apoptosis and the prevalence of apoptotic versus mitotic cells in the membrana granulosa of ovarian follicles during spontaneous and induced atresia in ewes. Biol Reprod 56:837–846.

Karpinich NO, Tafani M, Rothman RJ, Russo M a., Farber JL (2002) The course of etoposide-induced apoptosis from damage to DNA and p53 activation to mitochondrial release of cytochrome c. J Biol Chem 277:16547–16552.

Katti G, Ara SA, Shireen A (2011) Magnetic Resonance Imaging (MRI) – A Review. Int J Dent Clin 3:65–70.

Kaufmann a M, Firlik a D, Fukui MB, Wechsler LR, Jungries C a, Yonas H (1999) Ischemic core and penumbra in human stroke. Stroke 30:93–99.

Keen HG, Dekker B a., Disley L, Hastings D, Lyons S, Reader AJ, Ottewell P, Watson A, Zweit J (2005) Imaging apoptosis in vivo using 124I-annexin V and PET. Nucl Med Biol 32:395–402.

Kerr J, Wyllie A, Currie A (1972) Apoptosis: A basic biological phenomenon with wide-ranging implications in human disease. J Intern Med 258:479–517.

Khalil MM, Tremoleda JL, Bayomy TB, Gsell W (2011) Molecular SPECT Imaging: An Overview. Int J Mol Imaging 2011:796025.

Kischkel FC, Hellbardt S, Behrmann I, Germer M, Pawlita M, Krammer PH, Peter ME (1995) Cytotoxicity-dependent APO-1 (Fas/CD95)-associated proteins form a death-inducing signaling complex (DISC) with the receptor. EMBO J 14:5579–5588.

Koopman G, Reutelingsperger C, Kuijten G, Keehnen R, Pals S, Oers M va (1994) Annexin V for Flow Cytometric Detection of Phosphatidylserine Expression on B Cells Undergoing Apoptosis. Blood 84:1415–1420.

Kothakota S, Azuma T, Reinhard C, Klippel a, Tang J, Chu K, McGarry TJ, Kirschner MW, Koths K, Kwiatkowski DJ, Williams LT (1997) Caspase-3-generated fragment of gelsolin: effector of morphological change in apoptosis. Science 278:294–298.

Levine AJ (1997) P53, the Cellular Gatekeeper for Growth and Division. Cell 88:323–331.

Li H, Wang H, Liu S, Deng Y, Zhang Y, Tian Q, Wang X, Chen X, Yang Y, Zhang J, Wang Q, Xu H, Liao F, Wang J (2007) Phosphorylation of tau antagonizes apoptosis by stabilizing ␤-catenin , a mechanism involved in Alzheimer ' s neurodegeneration. Proc Natl Acad Sci 104:3591–3596.

Linnik MD, Miller J a, Sprinkle-Cavallo J, Mason PJ, Thompson FY, Montgomery LR, Schroeder KK (1995) Apoptotic DNA fragmentation in the rat cerebral cortex induced by permanent middle cerebral artery occlusion. Brain Res Mol Brain Res 32:116–124.

Liu J, Bhalgat M, Zhang C, Diwu Z, Hoyland B, Klaubert DH (1999) Fluorescent molecular probes V: a sensitive caspase-3 substrate for fluorometric assays. Bioorg Med Chem Lett 9:3231–3236.

Liu LF, Duann P, Lin CT, D'Arpa P, Wu J (1996) Mechanism of action of camptothecin. Ann N Y Acad Sci 803:44–49.

Loo DT, Copani a, Pike CJ, Whittemore ER, Walencewicz a J, Cotman CW (1993) Apoptosis is induced by beta-amyloid in cultured central nervous system neurons. Proc Natl Acad Sci U S A 90:7951–7955.

Lorberboym M, Blankenberg FG, Sadeh M, Lampl Y (2006) In vivo imaging of apoptosis in patients with acute stroke: Correlation with blood-brain barrier permeability. Brain Res 1103:13–19.

Love S (2003) Apoptosis and brain ischaemia. Prog Neuro-Psychopharmacology Biol Psychiatry 27:267–282.

Lowe MJ, Dzemidzic M, Lurito JT, Mathews VP, Phillips MD (2000) Correlations in low-frequency BOLD fluctuations reflect cortico-cortical connections. Neuroimage 12:582–587.

Luo Q-Y, Zhang Z-Y, Wang F, Lu H-K, Guo Y-Z, Zhu R-S (2005) Preparation, in vitro and in vivo evaluation of (99m)Tc-Annexin B1: a novel radioligand for apoptosis imaging. Biochem Biophys Res Commun 335:1102–1106.

Maheshwari SR, Fatterpekar GM, Castillo M, Mukherji SK (2000) Proton MR spectroscopy of the brain. Semin Ultrasound CT MR 21:434–451.

Majno G, Joris I (1995) Apoptosis, oncosis, and necrosis. An overview of cell death. Am J Pathol 146:3–15.

Mandl SJ, Mari C, Edinger M, Negrin RS, Tait JF, Contag CH, Blankenberg FG (2004) Multi-modality imaging identifies key times for annexin V imaging as an early predictor of therapeutic outcome. Mol Imaging 3:1–8.

Martin SJ, Reutelingsperger CP, McGahon a J, Rader J a, van Schie RC, LaFace DM, Green DR (1995) Early redistribution of plasma membrane phosphatidylserine is a general feature of apoptosis regardless of the initiating stimulus: inhibition by overexpression of Bcl-2 and Abl. J Exp Med 182:1545–1556.

Martinez MM, Reif RD, Pappas D (2010) Detection of apoptosis: A review of conventional and novel techniques. Anal Methods 2:996.

Masliah E, Mallory M, Alford M, Tanaka S, Hansen L (1998) Caspase dependent DNA fragmentation might be associated with excitotoxicity in Alzheimer disease. J Neuropathol Exp Neurol 57:1041–1052.

Mattson MP (2000) Apoptosis in neurodegenerative disorders. :120–129.

Mayeux R. Epidemiology of neurodegeneration. Annu Rev Neurosci 2003; 26: 81-104.

McIlwain DR, Berger T, Mak TW (2013) Caspase functions in cell death and disease. Cold Spring Harb Perspect Biol 5:1–28.

Medema JP, Scaffidi C, Kischkel FC, Shevchenko A, Mann M, Krammer PH, Peter ME (1997) FLICE is activated by association with the CD95 death-inducing signaling complex (DISC). EMBO J 16:2794–2804.

Messam C a, Pittman RN (1998) Asynchrony and commitment to die during apoptosis. Exp Cell Res 238:389–398.

Miura M (2011) Active participation of cell death in development and organismal homeostasis. Dev Growth Differ 53:125–136.

Mizutani H, Tada-Oikawa S, Hiraku Y, Kojima M, Kawanishi S (2005) Mechanism of apoptosis induced by doxorubicin through the generation of hydrogen peroxide. Life Sci 76:1439–1453.

Mochizuki H, Goto K, Mori H, Mizuno Y (1996) Histochemical detection of apoptosis in Parkinson's disease. J Neurol Sci 137:120–123.

Mori C, Nakamura N, Kimura S, Irie H, Takigawa T, Shiota K (1995) Programmed cell death in the interdigital tissue of the fetal mouse limb is apoptosis with DNA fragmentation. Anat Rec 242:103–110.

Morton CL, Houghton PJ (2007) Establishment of human tumor xenografts in immunodeficient mice. Nat Protoc 2:247–250.

Nair P, Lu M, Petersen S, Ashkenazi A (2014) Apoptosis initiation through the cell-extrinsic pathway, 1st ed. Elsevier Inc. Available at: http://dx.doi.org/10.1016/B978-0-12-417158-9.00005-4.

Nicholson DW (1999) Caspase structure, proteolytic substrates, and function during apoptotic cell death. Cell Death Differ 6:1028–1042.

Niu G, Chen X (2010) Apoptosis imaging: beyond annexin V. J Nucl Med 51:1659–1662.

O'Brien M a., Moravec R a., Riss L (2001) Poly (ADP-ribose) polymerase cleavage monitored in situ in apoptotic cells. Biotechniques 30:886–891.

Ogasawara J, Watanabe-Fukunaga R, Adachi M, Matsuzawa A, Kasugal T, Kitamura Y, Itoh N, Suda T, Nagata S (1993) Lethal effect of the anti-Fas antibody in mice. Nature 364:806–809.

Park JA, Lee JJ, Jung JC, Yu DY, Oh C, Ha S, Kim TJ, Chang Y (2008) Gd-DOTA conjugate of RGD as a potential tumor-targeting MRI contrast agent. Chembiochem 9:2811–2813.

Platt N, Da Silva RP, Gordon S (1998) Recognizing death: The phagocytosis of apoptotic cells. Trends Cell Biol 8:365–372.

Portera-Cailliau C, Hedreen JC, Price DL, Koliatsos VE (1995) Evidence for apoptotic cell death in Huntington disease and excitotoxic animal models. J Neurosci 15:3775–3787.

Querfurth HW, Laferla FM (2010) Alzheimer's Disease. :329–344.

Reddy PH, Williams M, Charles V, Garrett L, Pike-Buchanan L, Whetsell WO, Miller G, Tagle D a (1998) Behavioural abnormalities and selective neuronal loss in HD transgenic mice expressing mutated full-length HD cDNA. Nat Genet 20:198–202.

Roos R a C (2010) Huntington's disease: a clinical review. Orphanet J Rare Dis 5:40 Available at: http://www.ojrd.com/content/5/1/40.

Roos WP, Kaina B (2006) DNA damage-induced cell death by apoptosis. Trends Mol Med 12:440–450.

Rudin M, Weissleder R (2003) Molecular imaging in drug discovery and development. Nat Rev Drug Discov 2:123–131.

Sakahira H, Enari M, Nagata S (1998) Cleavage of CAD inhibitor in CAD activation and DNA degradation during apoptosis. Nature 391:96–99.

Saraste A, Pulkki K (2000) Morphologic and biochemical hallmarks of apoptosis. Cardiovasc Res 45:528–537.

Savill J (1997) Recognition and phagocytosis of cells undergoing apoptosis. Br Med Bull 53:491–508.

Savill J, Fadok V (2000) Corpse clearance defines the meaning of cell death. Nature 407:784–788.

Sheehan JP, Palmer PE, Helm G a, Tuttle JB (1997) MPP+ induced apoptotic cell death in SH-SY5Y neuroblastoma cells: an electron microscope study. J Neurosci Res 48:226–237.

Shiraishi H, Okamoto H, Yoshimura A, Yoshida H (2006) ER stress-induced apoptosis and caspase-12 activation occurs downstream of mitochondrial apoptosis involving Apaf-1. J Cell Sci 119:3958–3966.

Shmuel a (1992) Identification of Programmed Cell Death In Situ. Cell 119:493–501.

Silva MT (2010) Secondary necrosis: The natural outcome of the complete apoptotic program. FEBS Lett 584:4491–4499 Available at: http://dx.doi.org/10.1016/j.febslet.2010.10.046.

Slee EA, Harte MT, Kluck RM, Wolf BB, Casiano CA, Newmeyer DD, Wang H, Reed JC, Nicholson DW, Alnemri ES, Green DR, Martin SJ (1999) Ordering the Cytochrome c–initiated Caspase Cascade: Hierarchical Activation of Caspases-2, -3, -6, -7, -8, and -10 in a Caspase-9–dependent Manner. 144:281–292.

Srinivasan a, Roth K a, Sayers RO, Shindler KS, Wong a M, Fritz LC, Tomaselli KJ (1998) In situ immunodetection of activated caspase-3 in apoptotic neurons in the developing nervous system. Cell Death Differ 5:1004–1016.

Stennicke HR, Jürgensmeier JM, Shin H, Deveraux Q, Wolf BB, Yang X, Zhou Q, Ellerby HM, Ellerby LM, Bredesen D, Green DR, Reed JC, Froelich CJ, Salvesen GS (1998) Pro-caspase-3 is a major physiologic target of caspase-8. J Biol Chem 273:27084–27090.

Stennicke HR, Salvesen GS (1998) Properties of the caspases. Biochim Biophys Acta - Protein Struct Mol Enzymol 1387:17–31.

Su J, Anderson A, Cummings B, Cotman C (1994) Immunohistochemical evidence for apoptosis in Alzheimer's disease. Neuroreport 5:2529–2533.

Ta R, Suchy M, Tam JHK, Li AX, Martinez-Santiesteban FS, Scholl TJ, Hudson RHE, Bartha R, Pasternak SH (2013) A dual magnetic resonance imaging/fluorescent contrast agent for Cathepsin-D detection. Contrast Media Mol Imaging 8:127–139.

Tait JF (2008) Imaging of Apoptosis. J Nucl Med 49:1573–1576.

Tait JF, Gibson D, Fujikawa K (1989) Phospholipid binding properties of human placental anticoagulant protein-I, a member of the lipocortin family. J Biol Chem 264:7944–7949.

Tamaoki T, Nomoto H, Takahashi I, Kato Y, Morimoto M, Tomita F (1986) Staurosporine, a potent inhibitor of phospholipid/Ca++dependent protein kinase. Biochem Biophys Res Commun 135:397–402.

Tatton N a, Kish SJ (1997) In situ detection of apoptotic nuclei in the substantia nigra compacta of 1-methyl-4-phenyl-1,2,3,6-tetrahydropyridine-treated mice using terminal deoxynucleotidyl transferase labelling and acridine orange staining. Neuroscience 77:1037–1048.

Taylor RC, Cullen SP, Martin SJ (2008) Apoptosis: controlled demolition at the cellular level. Nat Rev Mol Cell Biol 9:231–241.

Tipton KF, Singer TP (1993) Advances in our understanding of the mechanisms of the neurotoxicity of MPTP and related compounds. J Neurochem 61:1191–1206.

Tremblay RG, Sikorska M, Sandhu JK, Lanthier P, Ribecco-Lutkiewicz M, Bani-Yaghoub M (2010) Differentiation of mouse Neuro 2A cells into dopamine neurons. J Neurosci Methods 186:60–67.

Trump BE, Berezesky IK, Seung H, Phelps PC (1997) Pathways Oncosis , Apoptosis , and Necrosis *. Toxicol Pathol 25:82–88.

Tsujimoto Y, Shimizu S (2007) Role of the mitochondrial membrane permeability transition in cell death. Apoptosis 12:835–840.

Van den Heuvel MP, Hulshoff Pol HE (2010) Exploring the brain network: A review on resting-state fMRI functional connectivity. Eur Neuropsychopharmacol 20:519–534 Available at: http://dx.doi.org/10.1016/j.euroneuro.2010.03.008.

Van Engeland M, Nieland LJW, Ramaekers FCS, Schutte B, Reutelingsperger CPM (1998) Annexin V-Affinity Assay: A review on an apoptosis detection system based on phosphatidyserine exposure. Cytometry 31:1–9.

Vernooij M, Smits M (2012) Structural neuroimaging in aging and Alzheimer's disease. Neuroimaging Clin N Am 22:33–55.

Viswanath V, Wu Y, Boonplueang R, Chen S, Stevenson FF, Yantiri F, Yang L, Beal MF, Andersen JK (2001) Caspase-9 activation results in downstream caspase-8 activation and bid cleavage in 1-methyl-4-phenyl-1,2,3,6-tetrahydropyridine-induced Parkinson's disease. J Neurosci 21:9519–9528.

Wadia JS, Chalmers-Redman RM, Ju WJ, Carlile GW, Phillips JL, Fraser a D, Tatton WG (1998) Mitochondrial membrane potential and nuclear changes in apoptosis caused by serum and nerve growth factor withdrawal: time course and modification by (-)-deprenyl. J Neurosci 18:932–947.

Wall ME, Wani MC (1996) Camptothecin. Discovery to clinic. Ann N Y Acad Sci 803:1–12.

Wang HH, Li HL, Liu R, Zhang Y, Liao K, Wang Q, Wang JZ, Liu SJ (2010) Tau overexpression inhibits cell apoptosis with the mechanisms involving multiple viability-related factors. J Alzheimer's Dis 21:167–179.

Wang Y, Qin Z-H (2010) Molecular and cellular mechanisms of excitotoxic neuronal death. Apoptosis 15:1382–1402.

Wang ZQ, Liao J, Diwu Z (2005) N-DEVD-N′-morpholinecarbonyl-rhodamine 110: Novel caspase-3 fluorogenic substrates for cell-based apoptosis assay. Bioorganic Med Chem Lett 15:2335–2338.

Watanabe M, Hitomi M, van der Wee K, Rothenberg F, Fisher S a, Zucker R, Svoboda KKH, Goldsmith EC, Heiskanen KM, Nieminen A-L (2002) The pros and cons of apoptosis assays for use in the study of cells, tissues, and organs. Microsc Microanal 8:375–391.

Watanabe Y, Himeda T, Araki T (2005) Mechanisms of MPTP toxicity and their implications for therapy of Parkinson's disease. Med Sci Monit 11:RA17–A23.

Watters D (1999) Molecular mechanisms of ionizing radiation-induced apoptosis. Immunol Cell Biol 77:263–271.

Weissleder R, Mahmood U (2001) Molecular Imaging. Radiology 219:316–333 Available at: http://www.ncbi.nlm.nih.gov/pubmed/11323453.

Wong RS (2011) Apoptosis in cancer: from pathogenesis to treatment. J Exp Clin Cancer Res 30:87 Available at: http://www.jeccr.com/content/30/1/87.

Wyllie a H, Morris RG, Smith a L, Dunlop D (1984) Chromatin cleavage in apoptosis: association with condensed chromatin morphology and dependence on macromolecular synthesis. J Pathol 142:67–77.

Ziegler U, Groscurth P (2004) Morphological features of cell death. News Physiol Sci 19:124–128.

Zimmermann KC, Green DR (2001) How cells die: Apoptosis pathways. J Allergy Clin Immunol 108:0–4.

Zou H, Li Y, Liu X, Wang X (1999) An APAf-1 ?? cytochrome C multimeric complex is a functional apoptosome that activates procaspase-9. J Biol Chem 274:11549–11556.

Appendix A

Western

AUP Number: 2009-099
PI Name: Cregan, Sean
AUP Title: The Mechanisms Of Neuronal Apoptosis In Vivo
Approval Date: 07/07/2014

Official Notice of Animal Use Subcommittee (AUS) Approval: Your new Animal Use Protocol (AUP) entitled "The Mechanisms Of Neuronal Apoptosis In Vivo" has been APPROVED by the Animal Use Subcommittee of the University Council on Animal Care. This approval, although valid for four years, and is subject to annual Protocol Renewal.2009-099::5

1. This AUP number must be indicated when ordering animals for this project.
2. Animals for other projects may not be ordered under this AUP number.
3. Purchases of animals other than through this system must be cleared through the ACVS office. Health certificates will be required.

The holder of this Animal Use Protocol is responsible to ensure that all associated safety components (biosafety, radiation safety, general laboratory safety) comply with institutional safety standards and have received all necessary approvals. Please consult directly with your institutional safety officers.

Submitted by: Copeman, Laura
on behalf of the Animal Use Subcommittee
University Council on Animal Care

Curriculum Vitae

Name: Mary Rebecca Cobb

Post-secondary Education and Degrees:

University of Western Ontario
London, Ontario, Canada
2009-2013 B.M.Sc.

University of Western Ontario
London, Ontario, Canada
2014-present M.Sc. Candidate

Honours and Awards:

Frederick Banting and Charles Best Canada Graduate Scholarship ($17,500 per annum): 2014-2015

Ontario Graduate Scholarship ($15,000 per annum): 2014-2015 (declined)

Poster Presentation at London Health Research Day (LHRD)
Top 80 Competitor
London, ON, Canada
April 2015
Developing a Contrast Agent for the *in Vivo* Detection of Apoptosis

Dean's Honor List: 2010-2013

Western Scholarship of Excellence: 2009

Related Work Experience

Teaching Assistant
The University of Western Ontario
2014-2015

Research Assistant
Robarts Research Institute
2013